

SSA: Sparse Sparse Attention by Aligning Full and Sparse Attention Outputs in Feature Space

Zhenyi Shen^{*†1,2} Junru Lu^{*2} Lin Gui¹ Jiazheng Li¹ Yulan He¹ Di Yin² Xing Sun²
¹King's College London ²Tencent Youtu Lab

Sparse attention reduces the quadratic complexity of full self-attention but faces two challenges: (1) an *attention gap*, where applying sparse attention to full-attention-trained models causes performance degradation due to train-inference distribution mismatch, and (2) a *capability gap*, where models trained purely with sparse attention lack complete gradient flow, preventing them from matching full-attention performance. We propose **SSA** (Sparse Sparse Attention), a training framework that integrates both sparse and full attention with bidirectional attention-output alignment. We prove that the approximation error scales linearly with the attention mass dropped under sparse attention, and show that SSA's alignment objective substantially reduces this quantity compared to baselines. Experiments demonstrate that SSA achieves state-of-the-art performance under both inference modes, adapts smoothly to varying sparsity budgets, and demonstrates superior long-context capabilities. The code is available at <https://github.com/zhenyi4/ssa>.

1 Introduction

With the blooming of large language models (LLMs), the demand for efficient long-context processing has grown substantially across diverse scenarios, including long-document understanding [Zhang et al., 2023, Jimenez et al., 2024], extended reasoning trajectories [OpenAI et al., 2024, DeepSeek-AI et al., 2025], and deep research workflows [Zheng et al., 2025]. The working length of LLMs has progressively expanded to 32K, 128K, and even to 1M tokens [Yang et al., 2025]. However, full self-attention in vanilla transformers exhibits quadratic computational complexity with respect to context length, rendering both training and inference prohibitive for such extended contexts.

To address quadratic complexity, existing studies [Sun et al., 2025] have investigated *sparse attention* mechanisms, which selectively restrict the number of tokens each query attends to, reducing the complexity to sub-quadratic. The goal is to achieve full-attention-level performance with the efficiency of sparse attention. However, two issues remain unsolved:

1) Attention Gap. Training-free methods directly apply sparse attention to models trained with full attention (**Full-Sparse**)¹ [Xiao et al., 2024, Jiang et al., 2024], exploiting inherent sparsity in attention. A metric for quantifying this approximation is **attention sparsity**: the proportion of total attention mass captured by selected tokens. We prove that the approximation error scales linearly with the dropped attention mass (Theorem 1), suggesting that higher attention sparsity yields closer approximation to full attention. However, the approximation error induced by the *mismatch between training and inference distributions* often incurs substantial performance degradation [Yuan et al., 2025].

2) Capability Gap. Trainable sparse attention methods train and deploy with sparse attention (**Sparse-Sparse**) [Yuan et al., 2025, Lu et al., 2025], eliminating the distribution mismatch. However, as full attention

^{*}Equal contribution.

[†]Work done during the internship at Tencent Youtu Lab.

¹(X-Y) denote attention configurations, where X and Y specify the attention mechanism used at training and inference, respectively.

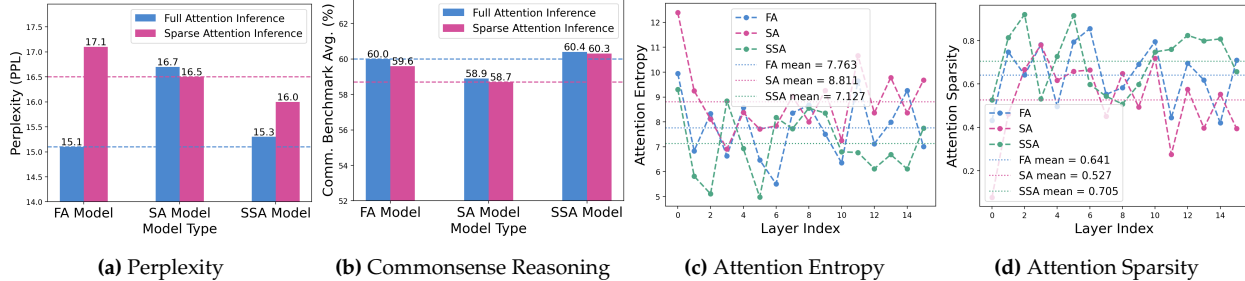


Figure 1. Performance and attention characteristics of 1B models. Under sparse inference, Sparse Attention Model (SA) achieves lower perplexity than Full Attention Model (FA) due to distribution mismatch, yet FA outperforms SA on benchmarks due to weaker training signals in SA. SSA resolves both issues, achieving the highest attention sparsity and best performance under both inference modes.

is not involved during training as a reference, the performance gap between sparse and full attention is never explicitly defined and cannot be bounded. Whether Sparse-Sparse models can match Full-Full performance relies entirely on an implicit assumption that both could achieve the same output behavior after training on the same data. However, this assumption is brittle: Sparse-Sparse models can only attend to a subset of preceding tokens, weakening both forward and backward signals compared to full attention and resulting in lower performance than Full-Full models [Lu et al., 2025].

To address these issues, we observe that training with sparse or full attention alone is insufficient. We propose **SSA** (Sparse Sparse Attention), a training framework that integrates both sparse and full attention while explicitly encouraging sparser attention distributions through attention-output alignment (Figure 2). At each training step, SSA randomly selects one of two attention modes with equal probability: **Sparse Attention** addresses the *Attention Gap* by directly optimizing for sparse inference, eliminating the train-inference distribution mismatch. **Full Attention** addresses the *Capability Gap* by providing complete gradient flow to all tokens, serving as a reference that enables attention sparsity to explicitly bound the approximation error. Furthermore, SSA computes the counterpart attention at each layer to perform bidirectional alignment, encouraging attention sparsity and tightening the bound: full-attention outputs are encouraged to match sparse-attention outputs, promoting inherently sparser distributions; sparse-attention outputs are regularized toward full-attention outputs, preventing drift from full-attention behavior.

SSA attains substantially higher attention sparsity than both Full-Full and Sparse-Sparse baselines, translating into strong performance under both inference modes (Figure 1). Our contributions are as follows:

- We establish a theoretical framework showing that pure full training induces an attention gap while pure sparse training induces a capability gap, and prove that the approximation error between sparse and full attention scales linearly with the dropped attention mass.
- We propose **SSA**, a unified training framework that integrates both sparse and full attention with bidirectional alignment, addressing both gaps while promoting inherently sparser attention distributions.
- Extensive experiments validate SSA achieves SOTA performance across multiple benchmarks, supports flexible inference under varying sparsity budgets, and delivers superior long-context performance.

2 Related Work

Training-Free Sparse Attention. Training-free sparse attention leverages the intrinsic sparsity in the attention distribution, allowing it to closely approximate full attention while significantly reducing computational cost. A widely used form is sliding-window attention, which restricts each token to attend only to its local

neighborhood [Child et al., 2019, Beltagy et al., 2020, Brown et al., 2020]. StreamingLLM [Xiao et al., 2024] further observes an “attention sink” phenomenon, where substantial attention mass is placed on the initial tokens, and incorporates these early tokens into the sparse attention set. Beyond fixed patterns, dynamic sparse attention selects informative segments based on the relevance between the query and attended keys. A common method is block-sparse attention [Xiao et al., 2024, Jiang et al., 2024, Xu et al., 2025, Tang et al., 2024, Zhang et al., 2025], which partitions the context into blocks, then selects the top- k important blocks for computation. In a nutshell, we categorize all training-free sparse attention methods as Full-Sparse type.

Trainable Sparse Attention. To further improve the effectiveness of sparse attention, MoBA [Lu et al., 2025] employs block-sparse attention during training, achieving performance comparable to full attention while being substantially more efficient. NSA [Yuan et al., 2025] integrates three complementary attention patterns: coarse global attention, block-sparse attention, and sliding-window attention, combined via a gating module. Although NSA reports performance surpassing full-attention models, subsequent analysis suggests that the improvement can be attributable to the additional gated-attention mechanism rather than the sparse design alone [Qiu et al., 2025]. Moreover, its multi-component structure makes it less flexible to adjust sparsity levels or revert to full attention at inference time. Concurrent to our work, InFLLM-v2 [Zhao et al., 2025] refines block selection through a two-level hierarchical mechanism. DSA [DeepSeek-AI, 2025] advances token retrieval by selecting top- k keys at token-level granularity rather than block-level. Although this approach still exhibits nominal $O(n^2)$ complexity, its cost is largely mitigated by highly optimized system implementations. In this work, we define the native sparse attention approaches as Sparse-Sparse paradigms.

In contrast to both Full-Sparse and Sparse-Sparse paradigms, SSA unifies sparse and full attention within a single framework while explicitly encouraging higher attention sparsity. This design enables the model to leverage the benefits of both paradigms during training and perform well under either inference mode.

3 Preliminary

Full Attention. In a standard transformer with softmax attention, each token attends to all preceding tokens:

$$h(t) = \text{softmax}[q(t)K^\top(: t)]V^\top(: t).$$

Here, t denotes the position of the query token, $q(t)$ is its query vector, K and V are the key and value matrices, $(\cdot)^\top$ denotes matrix transposition. Since all tokens in the context are used to predict the next token, we refer to this formulation as **Full Attention**. This operation has quadratic complexity with respect to context length, thus becoming prohibitive for a large number of context tokens.

Sparse Attention. To address this computational bottleneck, sparse attention restricts each query to attend only to a subset of preceding keys and values. In this work, we focus on *block-sparse attention*, where tokens are partitioned into contiguous blocks, and only tokens within selected blocks are attended to. Following MoBA [Lu et al., 2025], we compute the block-level keys by mean-pooling the token keys within each block. For each query, we compute dot-product similarities with all preceding block keys and select the top- k most relevant blocks. The tokens from selected blocks are concatenated to form reduced key and value matrices, denoted as \tilde{K} and \tilde{V} , yielding sparse attention:

$$\begin{aligned} \tilde{K} &= \{K(i) \mid i \in \text{Top-}k \text{ attention blocks}\}, \\ h(t) &= \text{softmax}[q(t)\tilde{K}^\top(: t)]\tilde{V}^\top(: t). \end{aligned}$$

A key characteristic of sparse attention is that attention only relies on partial token set. Given a sequence of length N partitioned into $n = N/s$ blocks of s tokens each, selecting k blocks yields a **receptive field** of ks tokens with a **sparsity ratio** of k/n . The resulting computational complexity becomes $\mathcal{O}(N \cdot ks) = \mathcal{O}(\frac{k}{n} \cdot N^2)$, reducing the quadratic cost of full attention proportionally to the sparsity ratio.

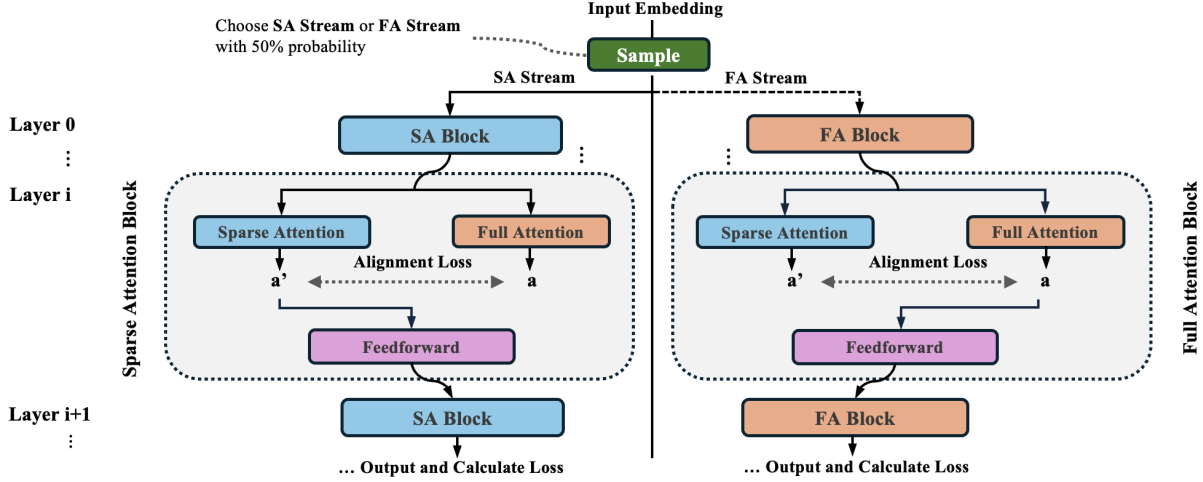


Figure 2. Illustration of the SSA training framework. At each iteration, the model has an equal probability of following either the Sparse Attention (SA) stream or the Full Attention (FA) stream. In the SA stream, the model learns sparse attention while aligning its output with a full-attention counterpart computed on the fly. Conversely, in the FA stream, the model learns full attention constrained by alignment with the corresponding sparse-attention output. For clarity, skip connections, normalization, and dropout layers are omitted in the figure.

Despite its favorable sub-quadratic scaling in long-context settings, sparse attention remains a performance bottleneck, both when used purely at inference time and when trained natively, due to the degradation in modeling quality observed in prior work [Lu et al., 2025, Yuan et al., 2025].

4 Theoretical Framework of Sparse Attention

We develop a theoretical framework explaining why neither pure sparse nor pure full attention training suffices, and derive conditions under which sparse attention closely approximates full attention. Our analysis reveals two insights: (1) exclusive sparse training causes gradient deficiencies while exclusive full training induces distribution mismatch; and (2) the approximation error scales linearly with dropped attention mass, motivating inherently sparser distributions.

4.1 Problem Setup

The goal of sparse attention is to approximate full attention performance while using fewer tokens for efficiency. Let $h_{\text{Tr}}^{\text{Inf}}(t)$ denote the attention hidden representation for query token t , where $\text{Tr} \in \{\text{FA}, \text{SA}\}$ indicates training with full or sparse attention, and $\text{Inf} \in \{\text{full}, \text{sparse}\}$ indicates the inference mechanism. Ideally, a well-trained sparse attention model should achieve:

$$\sum_{t=1}^T \|h_{\text{FA}}^{\text{full}}(t) - h_{\text{SA}}^{\text{sparse}}(t)\| < \epsilon, \quad (1)$$

for some small $\epsilon > 0$, where T denotes the sequence length.

4.2 Theoretical Framework

Capability Gap: Insufficiency of Sparse-Only Training. We identify two learning deficiencies induced by training exclusively with sparse attention.

Proposition 4.1 (Gradient Update Deficiency). *Training exclusively with sparse attention induces:*

1. **Learning Deficiency:** *For any token j in a dropped block, its gradient is zero, preventing the model from learning to attend to tokens outside the selected blocks.*
2. **Attention Suppression Deficiency:** *By excluding dropped tokens from the softmax denominator, SA models bypass the competitive pressure that forces FA models to learn globally contrastive attention distributions.*

These deficiencies indicate that sparse-trained models will: (1) underperform due to incomplete learning, and (2) fail to benefit from full attention at inference due to high-entropy attention patterns.

Attention Gap: Insufficiency of Full-Only Training. We formalize the distribution mismatch when training and inference use different attention mechanisms.

Proposition 4.2 (Attention Mechanism Alignment). *Let p_θ^{full} and p_θ^{sparse} denote the output token distributions under full and sparse attention, respectively. Let $\mathcal{L}_{\text{Tr}}^{\text{Inf}}$ denote the loss for a model trained with $\text{Tr} \in \{\text{FA, SA}\}$ and evaluated with $\text{Inf} \in \{\text{full, sparse}\}$. For a model trained only with full attention, sparse inference incurs an additional KL-divergence penalty:¹*

$$\mathcal{L}_{\text{FA}}^{\text{sparse}}(t) = \mathcal{L}_{\text{FA}}^{\text{full}}(t) + D_{\text{KL}}\left(p_\theta^{\text{full}}(t) \parallel p_\theta^{\text{sparse}}(t)\right). \quad (2)$$

In contrast, when training and inference use the same attention mechanism, no such penalty arises.

Remark 1. Although $\mathcal{L}_{\text{SA}}^{\text{sparse}} > \mathcal{L}_{\text{FA}}^{\text{full}}$ generally holds, a sufficiently large D_{KL} can yield $\mathcal{L}_{\text{SA}}^{\text{sparse}} < \mathcal{L}_{\text{FA}}^{\text{sparse}}$: a sparse-trained model achieves better perplexity under sparse inference than a full-trained model.

Propositions 4.1 and 4.2 collectively indicate that neither pure sparse nor pure full attention training suffices for high sparse-inference performance.

Quantifying the approximation error. To characterize whether sparse attention well-approximates full attention, we introduce a metric measuring the attention mass retained by sparse attention selection.

Definition 1 (Attention Sparsity). For query token t with attention weights $\{a(t, j)\}_{j < t}$, the *attention sparsity* is:

$$\text{AttnSparsity}(t) = \sum_{j < t} a(t, j) \cdot \mathbf{1}[\text{blk}(j) \in \mathcal{T}_k(t)], \quad (3)$$

where $\text{blk}(j)$ denotes the block index of token j , $\mathcal{T}_k(t)$ is the set of top- k blocks ranked by block-level attention scores, and $\mathbf{1}[\cdot]$ is the indicator function.

Higher attention sparsity indicates that sparse attention selection captures more of the total attention mass, suggesting closer approximation to full attention. We now bound the approximation error.

¹Proofs are provided in Appendix A.

Theorem 1 (Sparse Attention Error Bound). *Let $\mathcal{S}(t)$ denote the selected tokens and $\mathcal{S}^c(t)$ the dropped tokens. Define the dropped attention mass as $\delta(t) = \sum_{j \in \mathcal{S}^c(t)} a_j^{\text{full}}(t) = 1 - \text{AttnSparsity}(t)$. Then:²*

$$\|h^{\text{full}}(t) - h^{\text{sparse}}(t)\| \leq \delta(t) \left(\max_{j \in \mathcal{S}^c(t)} \|v(j)\| + \|h^{\text{sparse}}(t)\| \right), \quad (4)$$

where $v(j)$ denotes the value vector of token j .

Here, we didn't specify what kind of training attention well choose since it is a general result for either full-attention-trained or sparse-attention-trained models. This bound scales linearly with $\delta(t)$, motivating the learning of inherently sparser attention distributions to minimize approximation error under inference.

5 Sparse Sparse Attention (SSA)

From theory to method. Our theoretical analysis motivates decomposing the target gap (Equation 1) as:

$$\|h_{\text{FA}}^{\text{full}}(t) - h_{\text{SSA}}^{\text{sparse}}(t)\| \leq \underbrace{\|h_{\text{FA}}^{\text{full}}(t) - h_{\text{SSA}}^{\text{full}}(t)\|}_{\text{(I) Capability Gap}} + \underbrace{\|h_{\text{SSA}}^{\text{full}}(t) - h_{\text{SSA}}^{\text{sparse}}(t)\|}_{\text{(II) Attention Gap}}. \quad (5)$$

This motivates three design principles: (1) incorporate full attention training to minimize Term (I) (Proposition 4.1); (2) learn inherently sparser attention distributions to reduce Term (II) via the bound in Theorem 1; and (3) include sparse attention training to directly optimize for sparse inference (Proposition 4.2), improving performance beyond what the bound alone guarantees. Guided by these principles, we propose **SSA (Sparse Sparse Attention)** (Figure 2), a training framework that leverages the complementary strengths of sparse and full attention training while explicitly promoting attention sparsity, enabling sparse inference to match the capability of full-attention-trained models.

Dual-stream training. SSA alternates between full and sparse attention streams with equal probability. The full stream provides complete gradient flow to all tokens, addressing the learning deficiencies in Proposition 4.1 and minimizing Term (I). The sparse stream directly optimizes for sparse inference, eliminating the KL-divergence penalty in Proposition 4.2. By alternating rather than jointly computing both streams, we reduce computational cost by half while ensuring the model processes an equal number of tokens as the baselines for a fair comparison.

Counterpart attention alignment. To further reduce the *Attention Gap* (Term II), we enforce bidirectional alignment between the hidden representations produced by full and sparse attention. At each layer, we compute an auxiliary attention output using the counterpart attention mode—used only for alignment and not propagated to subsequent layers.

The alignment objective consists of two complementary components. A **sparsity loss** encourages full-attention outputs to mimic sparse-attention outputs:

$$\mathcal{L}_{\text{sparsity}} = \|h_{\text{full}} - \text{sg}(h_{\text{sparse}})\|, \quad (6)$$

²Proofs are provided in Appendix B.

where h_{full} and h_{sparse} are the hidden representations produced by full and sparse attention at a given layer, and $\text{sg}(\cdot)$ denotes the stop-gradient operator. By inherently promoting sparser attention distributions, this objective reduces the dropped attention mass $\delta(t)$ in Theorem 1, tightening the error bound on Term (II).

A **commitment loss** regularizes sparse-attention outputs to remain close to full-attention outputs:

$$\mathcal{L}_{\text{commit}} = \|h_{\text{sparse}} - \text{sg}(h_{\text{full}})\|, \quad (7)$$

This is analogous to the commitment loss in VQ-VAE [van den Oord et al., 2017] and KL regularization in RLHF [Ouyang et al., 2022], ensuring the sparse branch remains aligned with the representational space of full attention. In practice, we use SmoothL1 loss for both components [Girshick, 2015].

The total alignment loss combines both:

$$\mathcal{L}_{\text{align}} = \mathcal{L}_{\text{sparsity}} + \mathcal{L}_{\text{commit}}. \quad (8)$$

This bidirectional alignment encourages full attention to become inherently sparser (reducing $\delta(t)$) while keeping them stable. Notably, value-level alignment is substantially more efficient than directly aligning attention distributions, which would require materializing dense attention maps incompatible with FlashAttention-2 [Dao, 2024].

Overall objective. The final training objective combines cross-entropy loss with alignment:

$$\mathcal{L} = \mathbb{E}_{\text{mode} \sim \{\text{full}, \text{sparse}\}} [\mathcal{L}_{\text{ce}}^{\text{mode}}] + \alpha \mathcal{L}_{\text{align}}, \quad (9)$$

where $\mathcal{L}_{\text{ce}}^{\text{mode}}$ is the cross-entropy loss under the sampled attention mode, and α is a weighting coefficient. The full algorithm is detailed in Algorithm 1 in the appendix.

Efficiency analysis. During inference, SSA performs identical sparse attention operations to MoBA [Lu et al., 2025], achieving $\sim 2\times$ speedup over full attention at 128k context length (Table A3). During training, although auxiliary attention is computed at each layer, it is not propagated to subsequent layers, increasing cost only marginally ($\sim 17\%$, Table A2). More details are in Appendix D.

6 Experimental Setup

Pretraining Setup. We follow the architecture and configuration of Llama-3.2-1B [Grattafiori et al., 2024] with two minor modifications (details in Appendix C). The model is pretrained on the SmoILM corpus [allal et al., 2025] for 100B tokens with 8k context length, using a learning rate of 1e-3 with cosine decay and a global batch size of 3.15M tokens. To further assess long-context capability, we continue training for additional 10B tokens at 32k length with a RoPE scaling factor of 4, using data sampled from DCLM [Li et al., 2024].

Baselines. We compare SSA against the following baselines: (1) **FullAttn**: the standard full attention mechanism. (2) **MoBA** [Lu et al., 2025]: a trainable sparse attention method conceptually aligned with SSA’s Sparse Attention Stream. (3) **NSA** [Yuan et al., 2025]: a sparse attention framework with three components—compression, selection, and sliding window, aggregating them to form the final attention representation, where the selection module is analogous to MoBA. NSA has a larger effective receptive field than others: its compression module accesses the compressed representations of all tokens, and the sliding window attends to a fixed number of local tokens. For each baseline, we train two configurations: one with a receptive field of 1024 (block size 32, top-32 blocks, and one with a receptive field of 256 (block size 16, top-16 blocks). For SSA, we report the 1024-receptive-field results obtained by extrapolating the 256-receptive-field model, as that model consistently performs better, this is likely due to inducing higher sparsity regularisation (see Section 7.5 for details). For NSA, we set the window size as 128 for both configurations.

Table 1. Comparison of different attention training methods on commonsense reasoning and perplexity under both full and sparse attention inference. The receptive field denotes the maximum number of accessible tokens during sparse-attention inference. SSA consistently outperforms all other methods on the benchmarks on average across all levels of sparsity. All results are averaged over 5 runs.

Method	PIQA/%	HellaSwag/%	ARC-Easy/%	ARC-Challenge/%	Average/% \uparrow	Wikitext PPL \downarrow
Full Attention Inference						
FullAttn	74.17 \pm 0.37	58.22 \pm 0.14	69.29 \pm 0.55	38.35 \pm 0.38	60.01 \pm 0.19	15.13
MoBA	72.75 \pm 0.15	56.18 \pm 0.19	69.24 \pm 0.28	37.27 \pm 0.68	58.86 \pm 0.19	16.68
SSA	74.54 \pm 0.48	58.45 \pm 0.19	69.92 \pm 0.32	38.65 \pm 0.55	60.39 \pm 0.20	15.28
Sparse Attention Inference (Receptive Field = 256)						
FullAttn	74.23 \pm 0.39	57.84 \pm 0.20	68.84 \pm 0.20	37.56 \pm 0.55	59.62 \pm 0.31	17.05
MoBA	72.64 \pm 0.34	56.39 \pm 0.21	68.83 \pm 0.41	37.05 \pm 0.30	58.73 \pm 0.16	16.54
NSA	73.23 \pm 0.30	58.15 \pm 0.32	69.80 \pm 0.34	36.71 \pm 0.58	59.47 \pm 0.20	16.02
SSA	74.53 \pm 0.55	58.40 \pm 0.08	69.62 \pm 0.30	38.53 \pm 0.64	60.27 \pm 0.22	15.96
Sparse Attention Inference (Receptive Field = 1024)						
FullAttn	74.35 \pm 0.24	58.13 \pm 0.11	69.34 \pm 0.34	38.34 \pm 0.55	60.04 \pm 0.17	15.67
MoBA	72.99 \pm 0.26	56.26 \pm 0.15	69.16 \pm 0.37	36.14 \pm 0.33	58.64 \pm 0.14	16.02
NSA	73.57 \pm 0.29	58.39 \pm 0.08	70.07 \pm 0.21	38.69 \pm 0.49	60.18 \pm 0.15	15.48
SSA	74.53 \pm 0.10	58.50 \pm 0.11	69.97 \pm 0.29	38.57 \pm 0.51	60.39 \pm 0.15	15.51

Evaluation. We evaluate our models along two major dimensions. First, we assess performance on classical commonsense reasoning benchmarks: **PIQA** [Bisk et al., 2019], **Hellaswag** [Zellers et al., 2019], **ARC-Easy** [Clark et al., 2018], and **ARC-Challenge** [Clark et al., 2018]. On each benchmark, we run 5 different seeds and report the average. We additionally measure word perplexity on **WikiText** [Merity et al., 2017] with the context length capped at 8k. Second, we evaluate models on longer context tasks. Specifically, we use **LongBench** [Bai et al., 2024] (16 English benchmarks) to measure long-context understanding, **Needle-in-A-Haystack** from **RULER** [Hsieh et al., 2024] to assess retrieval, and **PG19** [Rae et al., 2020] to compute long-context perplexity, where PPL is obtained via sliding-window evaluation with a stride of 256 [Press et al., 2021, 2022]. All benchmarks are run using **lm-evaluate-harness** [Gao et al., 2024], and normalized accuracy is reported when applicable. All models are evaluated under both sparse and full attention modes at inference except NSA (discussed in Appendix F), enabling us to measure how well they generalize when given full KV-cache access. Unless otherwise specified, we use their receptive-field-256 variants for extrapolation. More details are shown in Appendix E.

7 Experimental Analysis

7.1 Language Modeling

In Table 1 (last column), SSA achieves the lowest perplexity under sparser attention (RF=256), though it slightly lags behind NSA at RF=1024 due to NSA’s sliding window module (see Appendix G). These results validate our theoretical framework. First, **supporting Proposition 4.2**, we observe that MoBA achieves lower PPL than FullAttn under sparse-inference, despite FullAttn’s full-inference performance. This confirms that pure full-attention training incurs a substantial distribution mismatch penalty when switching to sparse inference. Second, **supporting Theorem 1**, SSA exhibits a much smaller perplexity gap between sparse and full mode compared to FullAttn. As shown in Figure 1, SSA inherently learns sparser attention distributions, reducing the dropped attention mass $\delta(t)$ and thereby tightening the attention gap (Term II in Equation 5).

Third, SSA’s full-attention perplexity remains only marginally higher than FullAttn, indicating a small capability gap (Term I). Together, minimizing both terms yields SSA’s superior sparse-inference performance.

7.2 Commonsense Reasoning

As shown in Table 1 (left five columns), SSA in general consistently outperforms all baselines under the same sparsity budget, and notably surpasses FullAttn while using a receptive field of only 256. Under sparse attention, MoBA underperforms FullAttn, **validating Proposition 4.1** about the learning deficiency, while SSA successfully overcomes this limitation by incorporating full attention into training. Interestingly, SSA achieves better downstream benchmark performance than FullAttn under full attention, despite having higher perplexity in the same setting. Our ablation results (Table 2) explain this phenomenon: removing the alignment loss (NoAlignmentLoss) substantially degrades benchmark performance, while training with full attention only but retaining the alignment loss (FullRatio=1) preserves the gains. This suggests that the sparser attention distributions benefit downstream reasoning. A plausible explanation is that sparser attention encourages the model to focus on informative tokens while ignoring irrelevant ones.

Table 2. Ablation studies. $\text{train}A \times B$ denotes training with top-k A and block size B , while $\text{inf}A \times B$ indicate the inference setting. **FullRatio** notes the sampling ratio of the Full Attention Stream in Figure 2. **Only Full**→**Sparse** applies solo alignment from full attention to sparse attention, while **Only Sparse**→**Full** applies solo alignment reversely.

Method	PPL \downarrow	Comm. Avg. \uparrow
Baseline (SSA)	24.20	49.69
MoBA	24.51	48.81
Sparsity Level		
Baseline($\text{inf}8 \times 16$)	25.26	49.69
train8×16	25.97	48.88
Baseline($\text{inf}16 \times 32$)	23.52	49.78
train16×32	23.60	49.32
Baseline($\text{inf}16 \times 64$)	23.23	49.96
train16×64	23.22	49.16
Sampling Ratio to the Full Attention Stream		
FullRatio=1	25.16	49.58
FullRatio=0.75	24.27	49.66
FullRatio=0.5 (Baseline)	24.20	49.69
FullRatio=0.25	24.32	49.25
FullRatio=0	24.40	49.00
Random Each Layer	NaN	0.00
Alignment Loss		
Only Full→Sparse	NaN	0.00
Only Sparse→Full	NaN	0.00
No Alignment Loss	24.48	48.38

7.3 Extrapolation between Different Levels of Sparsity

SSA extrapolates effectively across sparsity levels, exhibiting largely monotonic performance improvement across all four tasks as more tokens are included in sparse-attention computation (Figure 3). In contrast, MoBA fails to extrapolate on Perplexity and LongBench, and degrades at a receptive field of 4096 for

Commonsense and NIAH. We attribute this to MoBA’s insufficiently sparse attention distribution: when additional tokens become available, irrelevant tokens are not adequately suppressed, introducing noise rather than useful context. FullAttn exhibits similar extrapolation to SSA but performs worse at nearly all sparsity levels, indicating that SSA’s higher attention sparsity bounds the gap between sparse and full attention more tightly.

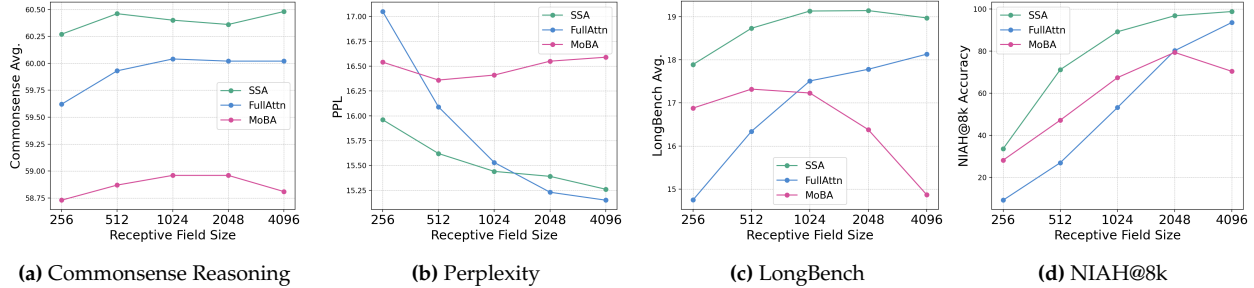


Figure 3. Performance versus receptive-field size. SSA and FullAttn extrapolate well as more tokens become visible, whereas MoBA exhibits poor extrapolation. We scale the receptive field by fixing block size and varying top-k. Detailed scores are in Appendix I.

7.4 Long Context Evaluation

Language Modeling. On longer context tasks, Figure 4 shows that SSA consistently outperforms baselines under sparse attention on PG-19, consistent with the results in Table 1. Under full attention without continued training, SSA surprisingly outperforms FullAttn (Figure 4a), reversing the trend from Table 1. We attribute this to SSA’s sparser attention distribution (Table A16): sparse attention patterns are more robust to RoPE scaling degradation, as evidenced by the smaller gap between RoPE-scaled and 32k-trained curves under sparse inference modes. Intuitively, attending to fewer and more local tokens reduces sensitivity to positional distortions introduced by RoPE scaling (see Appendix L for details). After continued training, FullAttn recovers and surpasses SSA under full attention, though SSA retains its advantage under sparse inference.

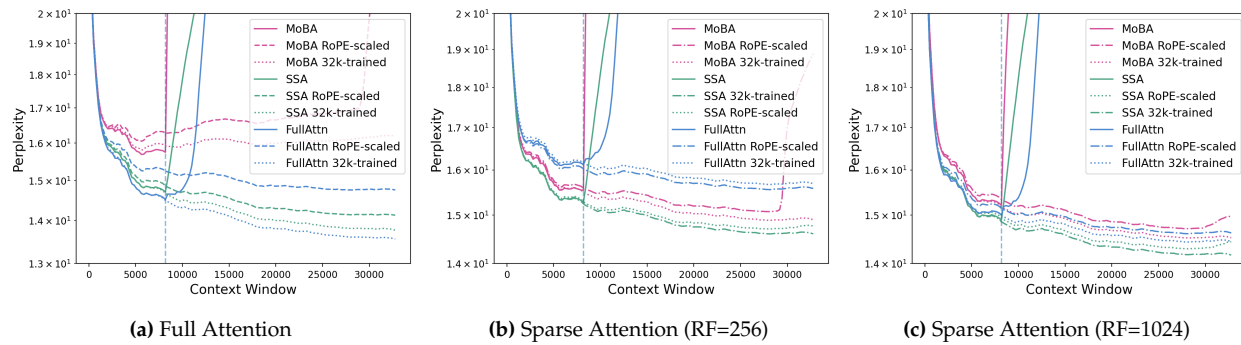


Figure 4. Perplexity across context lengths under different inference modes tested on PG-19. SSA achieves the lowest perplexity under sparse attention inference and exhibits the strongest robustness to RoPE scaling under full attention.

Needle-in-a-Haystack (NIAH). In Table 3, SSA is the strongest sparse attention method within 8k context length across all receptive fields and achieves 100% accuracy under full attention inference. This strong performance stems from SSA’s alignment training: within 8k, full attention provides global awareness that guides sparse attention’s feature learning and ranking, enabling reliable retrieval from arbitrary positions. Beyond 8k, SSA’s performance decreases as this regime lies outside the alignment training distribution. In contrast, MoBA shows stronger retrieval at longer contexts due to its purely content-based block selection, which is more position-agnostic and thus generalizes better to out-of-distribution distances. Nevertheless,

Table 3. Evaluation in longer context lengths. Left: length extrapolation to 32K using RoPE scaling on models pretrained up to 8K tokens. Right: models continually trained to 32K tokens. SSA outperforms all baselines on LongBench and NIAH under all modes, except for NIAH under full-attention inference with continual training. Best results are **bolded**; full LongBench results are provided in Appendix J.

Inference Mode	Receptive Field	Method	Length Extrapolation (RoPE Scaling)						Continual Trained to 32k					
			Needle in A Haystack/%					LongBench/%	Needle in A Haystack/%					LongBench/%
			4k	8k	16k	32k	Avg	32k	4k	8k	16k	32k	Avg	32k
Full Attention	Full	FullAttn	100	100	48	35.4	70.9	17.71	100	100	99.2	93.2	98.1	18.97
		MoBA	100	32.4	2.2	0	33.7	13.62	99	73.2	5.4	1.2	44.7	14.47
		SSA	100	100	83	35.4	79.6	18.32	100	100	99.8	70.6	92.6	19.55
Sparse Attention	256	FullAttn	48	9.2	4.2	2.8	16.1	14.75	53	11.8	5.4	3.6	18.5	14.96
		MoBA	68.8	28.2	14.4	0	27.9	16.88	82	27.6	12.4	3	31.3	17.17
		NSA	37.4	13.8	3.6	2.4	14.3	17.25	61	34.2	5.4	4.8	26.4	17.45
		SSA	81.6	33.6	5.8	2.2	30.8	17.89	89.2	34.8	7.8	3.2	33.8	18.25
Sparse Attention	1024	FullAttn	58.2	21.4	7.2	4.4	22.8	16.72	59	25	9.2	5.2	24.6	16.84
		MoBA	58.4	27.8	16	8	27.6	18.23	93.8	36.2	17.6	9.4	39.3	18.68
		NSA	64.6	25	11.4	4	26.3	17.36	74.4	27.8	10.6	6.6	29.9	18.08
		SSA	77.4	47.8	10	3.8	34.8	18.58	94	55.6	17.2	5.4	43.1	19.05

SSA maintains superior full-attention NIAH, whereas MoBA cannot effectively leverage full attention at inference. On average, SSA achieves the best performance in 5 out of 6 settings, offering practitioners the flexibility to choose sparse mode for efficiency or full attention for retrieval-intensive tasks.

LongBench. While perplexity and NIAH offer useful long-context diagnostics, they do not fully capture real-world long-context understanding: perplexity measures average prediction quality, and NIAH tests retrieval of a single fact. LongBench provides a more comprehensive evaluation across diverse tasks, requiring reasoning over long documents. Results from Table 3 confirm that SSA achieves the best performance across all inference modes and context extension settings on LongBench.

7.5 Ablation Studies

We ablate SSA along several dimensions. All experiments are conducted with 300M-parameter models (Table A1) trained on 50B tokens. More ablations in Appendix K.

Sparsity Levels. We observe that training with a larger receptive field (e.g., 16x32 or 16x64) does not improve SSA performance (Table 2). We hypothesize that a smaller receptive field imposes stronger structural constraints, providing more effective regularization for learning sparse attention patterns. Conversely, shrinking the receptive field too aggressively (e.g., 8x16) also fails to yield further benefits. These results suggest that an optimal receptive-field “sweet spot” is needed for the best performance.

Sampling Ratio to the Full Attention Stream. We vary the mixing ratio between the FA and SA streams. Moderate inclusion of the SA stream (e.g., FullRatio = 0.75) provides near-optimal perplexity, while placing more weight on the FA stream generally yields better downstream benchmark results. Eliminating either stream leads to noticeable performance degradation.

Alignment Loss. Without the alignment loss $L_{\text{alignment}}$ performance drops considerably. We hypothesize that Full Attention and Sparse Attention prefer different model weights for best performance, abruptly switching between them harms stability. Using only one direction of the alignment loss also results in unstable training.

We speculate this is due to asymmetric over-distillation: Full→Sparse forces the full attention path to overfit sparse patterns, degrading full-attention capability, while Sparse→Full has the opposite issue. Bi-directional alignment is therefore necessary to stabilize training.

8 Conclusion

We identified a critical paradox in sparse-attention training: native sparse-attention methods unexpectedly exhibit *insufficient* attention sparsity due to gradient-update deficiency on excluded key-value pairs. To address this, we proposed **SSA**, a unified framework that jointly aligns sparse and full attention bidirectionally. SSA achieves the highest attention sparsity among all methods, delivers superior performance on perplexity and downstream tasks in both sparse and full inference modes, and demonstrates strong robustness across different sparsity levels. Moreover, we show that sparse-attention-trained models exhibit stronger long-context extrapolation than full-attention models, with SSA achieving the best results on long-context understanding. Our work reveals that encouraging high attention sparsity during training benefits not only sparse-attention inference but also full-attention inference, opening new directions for designing scalable, efficient long-context LLMs that maintain high utility under diverse computational budgets.

9 Contact Information

Emails: Zhenyi Shen: zhenyi.shen@kcl.ac.uk, Junru Lu: junrulu@tencent.com

References

- [1] Fengji Zhang, Bei Chen, Yue Zhang, Jacky Keung, Jin Liu, Daoguang Zan, Yi Mao, Jian-Guang Lou, and Weizhu Chen. RepoCoder: Repository-level code completion through iterative retrieval and generation. In Houda Bouamor, Juan Pino, and Kalika Bali, editors, *Proceedings of the 2023 Conference on Empirical Methods in Natural Language Processing*, pages 2471–2484, Singapore, December 2023. Association for Computational Linguistics. doi: 10.18653/v1/2023.emnlp-main.151. URL <https://aclanthology.org/2023.emnlp-main.151/>.
- [2] Carlos E Jimenez, John Yang, Alexander Wettig, Shunyu Yao, Kexin Pei, Ofir Press, and Karthik R Narasimhan. SWE-bench: Can language models resolve real-world github issues? In *The Twelfth International Conference on Learning Representations*, 2024. URL <https://openreview.net/forum?id=VTF8yNQM66>.
- [3] OpenAI, :, Aaron Jaech, Adam Kalai, Adam Lerer, Adam Richardson, Ahmed El-Kishky, Aiden Low, Alec Helyar, Aleksander Madry, and et al. Openai o1 system card, 2024. URL <https://arxiv.org/abs/2412.16720>.
- [4] DeepSeek-AI, Daya Guo, Dejian Yang, Haowei Zhang, Junxiao Song, Ruoyu Zhang, Runxin Xu, Qihao Zhu, and et al. Deepseek-r1: Incentivizing reasoning capability in llms via reinforcement learning, 2025. URL <https://arxiv.org/abs/2501.12948>.
- [5] Yuxiang Zheng, Dayuan Fu, Xiangkun Hu, Xiaojie Cai, Lyumanshan Ye, Pengrui Lu, and Pengfei Liu. DeepResearcher: Scaling deep research via reinforcement learning in real-world environments. In *Proceedings of the 2025 Conference on Empirical Methods in Natural Language Processing*, 2025. doi: 10.18653/v1/2025.emnlp-main.22. URL <https://aclanthology.org/2025.emnlp-main.22/>.

- [6] An Yang, Bowen Yu, Chengyuan Li, Dayiheng Liu, Fei Huang, Haoyan Huang, Jiandong Jiang, Jianhong Tu, Jianwei Zhang, Jingren Zhou, Junyang Lin, Kai Dang, Kexin Yang, Le Yu, Mei Li, Minmin Sun, Qin Zhu, Rui Men, Tao He, Weijia Xu, Wenbiao Yin, Wenyuan Yu, Xiafei Qiu, Xingzhang Ren, Xinlong Yang, Yong Li, Zhiying Xu, and Zipeng Zhang. Qwen2.5-1m technical report, 2025. URL <https://arxiv.org/abs/2501.15383>.
- [7] Yutao Sun, Zhenyu Li, Yike Zhang, Tengyu Pan, Bowen Dong, Yuyi Guo, and Jianyong Wang. Efficient attention mechanisms for large language models: A survey, 2025. URL <https://arxiv.org/abs/2507.19595>.
- [8] Chaojun Xiao, Pingle Zhang, Xu Han, Guangxuan Xiao, Yankai Lin, Zhengyan Zhang, Zhiyuan Liu, and Maosong Sun. InfLLM: Training-free long-context extrapolation for LLMs with an efficient context memory. In *The Thirty-eighth Annual Conference on Neural Information Processing Systems*, 2024. URL <https://openreview.net/forum?id=bTHFrqhASY>.
- [9] Guangxuan Xiao, Yuandong Tian, Beidi Chen, Song Han, and Mike Lewis. Efficient streaming language models with attention sinks. In *The Twelfth International Conference on Learning Representations*, 2024. URL <https://openreview.net/forum?id=NG7sS51zVF>.
- [10] Huiqiang Jiang, YUCHENG LI, Chengruidong Zhang, Qianhui Wu, Xufang Luo, Surin Ahn, Zhenhua Han, Amir H. Abdi, Dongsheng Li, Chin-Yew Lin, Yuqing Yang, and Lili Qiu. MInference 1.0: Accelerating pre-filling for long-context LLMs via dynamic sparse attention. In *The Thirty-eighth Annual Conference on Neural Information Processing Systems*, 2024. URL <https://openreview.net/forum?id=fPBACAbqSN>.
- [11] Jingyang Yuan, Huazuo Gao, Damai Dai, Junyu Luo, Liang Zhao, Zhengyan Zhang, Zhenda Xie, Yuxing Wei, Lean Wang, Zhiping Xiao, Yuqing Wang, Chong Ruan, Ming Zhang, Wenfeng Liang, and Wangding Zeng. Native sparse attention: Hardware-aligned and natively trainable sparse attention. In Wanxiang Che, Joyce Nabende, Ekaterina Shutova, and Mohammad Taher Pilehvar, editors, *Proceedings of the 63rd Annual Meeting of the Association for Computational Linguistics (Volume 1: Long Papers)*, pages 23078–23097, Vienna, Austria, July 2025. Association for Computational Linguistics. ISBN 979-8-89176-251-0. doi: 10.18653/v1/2025.acl-long.1126. URL <https://aclanthology.org/2025.acl-long.1126>.
- [12] Enzhe Lu, Zhejun Jiang, Jingyuan Liu, Yulun Du, Tao Jiang, Chao Hong, Shaowei Liu, Weiran He, Enming Yuan, Yuzhi Wang, Zhiqi Huang, Huan Yuan, Suting Xu, Xinran Xu, Guokun Lai, Yanru Chen, Huabin Zheng, Junjie Yan, Jianlin Su, Yuxin Wu, Yutao Zhang, Zhilin Yang, Xinyu Zhou, Mingxing Zhang, and Jiezhong Qiu. MoBA: Mixture of block attention for long-context LLMs. In *The Thirty-ninth Annual Conference on Neural Information Processing Systems*, 2025. URL <https://openreview.net/forum?id=R1qYCpTu1P>.
- [13] Rewon Child, Scott Gray, Alec Radford, and Ilya Sutskever. Generating long sequences with sparse transformers, 2019. URL <https://arxiv.org/abs/1904.10509>.
- [14] Iz Beltagy, Matthew E. Peters, and Arman Cohan. Longformer: The long-document transformer, 2020. URL <https://arxiv.org/abs/2004.05150>.
- [15] Tom Brown, Benjamin Mann, Nick Ryder, Melanie Subbiah, Jared D Kaplan, Prafulla Dhariwal, Arvind Neelakantan, Pranav Shyam, Girish Sastry, Amanda Askell, Sandhini Agarwal, Ariel Herbert-Voss, Gretchen Krueger, Tom Henighan, Rewon Child, Aditya Ramesh, Daniel Ziegler, Jeffrey Wu, Clemens Winter, Chris Hesse, Mark Chen, Eric Sigler, Mateusz Litwin, Scott Gray, Benjamin Chess, Jack Clark, Christopher Berner, Sam McCandlish, Alec Radford, Ilya Sutskever, and Dario Amodei. Language models are few-shot learners. In *Advances in Neural Information Processing Systems*, 2020. URL https://proceedings.neurips.cc/paper_files/paper/2020/file/1457c0d6bfc4967418bfb8ac142f64a-Paper.pdf.
- [16] Ruyi Xu, Guangxuan Xiao, Haofeng Huang, Junxian Guo, and Song Han. XAttention: Block sparse attention with antidiagonal scoring. In *Forty-second International Conference on Machine Learning*, 2025. URL <https://openreview.net/forum?id=KG6aBfGi6e>.

[17] Jiaming Tang, Yilong Zhao, Kan Zhu, Guangxuan Xiao, Baris Kasikci, and Song Han. Quest: Query-aware sparsity for efficient long-context llm inference. In *ICML*, 2024. URL <https://openreview.net/forum?id=KzACYw0MTV>.

[18] Jintao Zhang, Chendong Xiang, Haofeng Huang, Jia wei, Haocheng Xi, Jun Zhu, and Jianfei Chen. Spargeattention: Accurate and training-free sparse attention accelerating any model inference. In *Forty-second International Conference on Machine Learning*, 2025. URL <https://openreview.net/forum?id=74c3Wwk8Tc>.

[19] Zihan Qiu, Zekun Wang, Bo Zheng, Zeyu Huang, Kaiyue Wen, Songlin Yang, Rui Men, Le Yu, Fei Huang, Suozhi Huang, Dayiheng Liu, Jingren Zhou, and Junyang Lin. Gated attention for large language models: Non-linearity, sparsity, and attention-sink-free. In *The Thirty-ninth Annual Conference on Neural Information Processing Systems*, 2025. URL <https://openreview.net/forum?id=1b7wh04SfY>.

[20] Weilin Zhao, Zihan Zhou, Zhou Su, Chaojun Xiao, Yuxuan Li, Yanghao Li, Yudi Zhang, Weilun Zhao, Zhen Li, Yuxiang Huang, Ao Sun, Xu Han, and Zhiyuan Liu. Inflilm-v2: Dense-sparse switchable attention for seamless short-to-long adaptation, 2025. URL <https://arxiv.org/abs/2509.24663>.

[21] DeepSeek-AI. Deepseek-v3.2-exp: Boosting long-context efficiency with deepseek sparse attention, 2025.

[22] Aaron van den Oord, Oriol Vinyals, and koray kavukcuoglu. Neural discrete representation learning. In I. Guyon, U. Von Luxburg, S. Bengio, H. Wallach, R. Fergus, S. Vishwanathan, and R. Garnett, editors, *Advances in Neural Information Processing Systems*, volume 30. Curran Associates, Inc., 2017. URL https://proceedings.neurips.cc/paper_files/paper/2017/file/7a98af17e63a0ac09ce2e96d03992fbc-Paper.pdf.

[23] Long Ouyang, Jeffrey Wu, Xu Jiang, Diogo Almeida, Carroll Wainwright, Pamela Mishkin, Chong Zhang, Sandhini Agarwal, Katarina Slama, Alex Ray, John Schulman, Jacob Hilton, Fraser Kelton, Luke Miller, Maddie Simens, Amanda Askell, Peter Welinder, Paul F Christiano, Jan Leike, and Ryan Lowe. Training language models to follow instructions with human feedback. In S. Koyejo, S. Mohamed, A. Agarwal, D. Belgrave, K. Cho, and A. Oh, editors, *Advances in Neural Information Processing Systems*, volume 35, pages 27730–27744. Curran Associates, Inc., 2022.

[24] Ross Girshick. Fast r-cnn, 2015. URL <https://arxiv.org/abs/1504.08083>.

[25] Tri Dao. Flashattention-2: Faster attention with better parallelism and work partitioning. In *The Twelfth International Conference on Learning Representations*, 2024. URL <https://openreview.net/forum?id=mZn2Xyh9Ec>.

[26] Aaron Grattafiori, Abhimanyu Dubey, Abhinav Jauhri, Abhinav Pandey, and et al. The llama 3 herd of models, 2024. URL <https://arxiv.org/abs/2407.21783>.

[27] Loubna Ben allal, Anton Lozhkov, Elie Bakouch, Gabriel Martin Blazquez, Guilherme Penedo, Lewis Tunstall, Andrés Marafioti, Agustín Piqueres Lajarín, Hynek Kydlíček, Vaibhav Srivastav, Joshua Lochner, Caleb Fahlgren, Xuan Son NGUYEN, Ben Burtenshaw, Clémentine Fourrier, Haojun Zhao, Hugo Larcher, Mathieu Morlon, Cyril Zakka, Colin Raffel, Leandro Von Werra, and Thomas Wolf. SmolLM2: When smol goes big — data-centric training of a fully open small language model. In *Second Conference on Language Modeling*, 2025. URL <https://openreview.net/forum?id=3JiCl2A14H>.

[28] Jeffrey Li, Alex Fang, Georgios Smyrnis, Maor Ivgi, Matt Jordan, Samir Yitzhak Gadre, Hritik Bansal, Etash Kumar Guha, Sedrick Keh, Kushal Arora, Saurabh Garg, Rui Xin, Niklas Muennighoff, Reinhard Heckel, Jean Mercat, Mayee F Chen, Suchin Gururangan, Mitchell Wortsman, Alon Albalak, Yonatan Bitton, Marianna Nezhurina, Amro Kamal Mohamed Abbas, Cheng-Yu Hsieh, Dhruba Ghosh, Joshua P Gardner, Maciej Kilian, Hanlin Zhang, Rulin Shao, Sarah M Pratt, Sunny Sanyal, Gabriel Ilharco, Giannis Daras, Kalyani Marathe, Aaron Gokaslan, Jieyu Zhang, Khyathi Chandu, Thao Nguyen, Igor Vasiljevic, Sham M. Kakade, Shuran Song, Sujay Sanghavi, Fartash Faghri, Sewoong Oh, Luke Zettlemoyer, Kyle Lo, Alaaeldin El-Nouby, Hadi Pouransari, Alexander T Toshev, Stephanie Wang, Dirk Groeneveld, Luca

Soldaini, Pang Wei Koh, Jenia Jitsev, Thomas Kollar, Alex Dimakis, Yair Carmon, Achal Dave, Ludwig Schmidt, and Vaishaal Shankar. Datacomp-LM: In search of the next generation of training sets for language models. In *The Thirty-eight Conference on Neural Information Processing Systems Datasets and Benchmarks Track*, 2024. URL <https://openreview.net/forum?id=CNWdWn47IE>.

[29] Yonatan Bisk, Rowan Zellers, Ronan Le Bras, Jianfeng Gao, and Yejin Choi. Piqa: Reasoning about physical commonsense in natural language, 2019. URL <https://arxiv.org/abs/1911.11641>.

[30] Rowan Zellers, Ari Holtzman, Yonatan Bisk, Ali Farhadi, and Yejin Choi. HellaSwag: Can a machine really finish your sentence? In *Proceedings of the 57th Annual Meeting of the Association for Computational Linguistics*, 2019. doi: 10.18653/v1/P19-1472. URL <https://aclanthology.org/P19-1472/>.

[31] Peter Clark, Isaac Cowhey, Oren Etzioni, Tushar Khot, Ashish Sabharwal, Carissa Schoenick, and Oyvind Tafjord. Think you have solved question answering? try arc, the ai2 reasoning challenge, 2018. URL <https://arxiv.org/abs/1803.05457>.

[32] Stephen Merity, Caiming Xiong, James Bradbury, and Richard Socher. Pointer sentinel mixture models. In *International Conference on Learning Representations*, 2017. URL <https://openreview.net/forum?id=Byj72udxe>.

[33] Yushi Bai, Xin Lv, Jiajie Zhang, Hongchang Lyu, Jiankai Tang, Zhidian Huang, Zhengxiao Du, Xiao Liu, Aohan Zeng, Lei Hou, Yuxiao Dong, Jie Tang, and Juanzi Li. LongBench: A bilingual, multitask benchmark for long context understanding. In Lun-Wei Ku, Andre Martins, and Vivek Srikumar, editors, *Proceedings of the 62nd Annual Meeting of the Association for Computational Linguistics (Volume 1: Long Papers)*, pages 3119–3137, Bangkok, Thailand, August 2024. Association for Computational Linguistics. doi: 10.18653/v1/2024.acl-long.172. URL [https://aclanthology.org/2024.acl-long.172/](https://aclanthology.org/2024.acl-long.172).

[34] Cheng-Ping Hsieh, Simeng Sun, Samuel Kriman, Shantanu Acharya, Dima Rekesh, Fei Jia, and Boris Ginsburg. RULER: What's the real context size of your long-context language models? In *First Conference on Language Modeling*, 2024. URL <https://openreview.net/forum?id=kIoBbc76Sy>.

[35] Jack W. Rae, Anna Potapenko, Siddhant M. Jayakumar, Chloe Hillier, and Timothy P. Lillicrap. Compressive transformers for long-range sequence modelling. In *International Conference on Learning Representations*, 2020. URL <https://openreview.net/forum?id=SylKikSYDH>.

[36] Ofir Press, Noah A. Smith, and Mike Lewis. Shortformer: Better language modeling using shorter inputs. In Chengqing Zong, Fei Xia, Wenjie Li, and Roberto Navigli, editors, *Proceedings of the 59th Annual Meeting of the Association for Computational Linguistics and the 11th International Joint Conference on Natural Language Processing (Volume 1: Long Papers)*, pages 5493–5505, Online, August 2021. Association for Computational Linguistics. doi: 10.18653/v1/2021.acl-long.427. URL [https://aclanthology.org/2021.acl-long.427/](https://aclanthology.org/2021.acl-long.427).

[37] Ofir Press, Noah Smith, and Mike Lewis. Train short, test long: Attention with linear biases enables input length extrapolation. In *International Conference on Learning Representations*, 2022. URL <https://openreview.net/forum?id=R8sQPpGCv0>.

[38] Leo Gao, Jonathan Tow, Baber Abbasi, Stella Biderman, Sid Black, Anthony DiPofi, Charles Foster, Laurence Golding, Jeffrey Hsu, Alain Le Noac'h, Haonan Li, Kyle McDonell, Niklas Muennighoff, Chris Ociepa, Jason Phang, Laria Reynolds, Hailey Schoelkopf, Aviya Skowron, Lintang Sutawika, Eric Tang, Anish Thite, Ben Wang, Kevin Wang, and Andy Zou. The language model evaluation harness, 07 2024. URL <https://zenodo.org/records/12608602>.

[39] Pin-Lun Hsu, Yun Dai, Vignesh Kothapalli, Qingquan Song, Shao Tang, Siyu Zhu, Steven Shimizu, Shivam Sahni, Haowen Ning, Yanning Chen, and Zhipeng Wang. Liger-kernel: Efficient triton kernels for LLM training. In *Championing Open-source DEvelopment in ML Workshop @ ICML25*, 2025. URL <https://openreview.net/forum?id=36SjAIT42G>.

A Proof of Proposition 4.2

Proof. Let's define the loss function based on the NLL (Negative Log Likelihood), where:

$$\begin{aligned}\mathcal{L}_{\text{FA}}^{\text{sparse}}(t) &= \mathbb{E}_{\text{FA}}[-\log p_{\theta}^{\text{sparse}}(t)], \\ \mathcal{L}_{\text{FA}}^{\text{full}}(t) &= \mathbb{E}_{\text{FA}}[-\log p_{\theta}^{\text{full}}(t)].\end{aligned}$$

Here, $\mathbb{E}_{\text{FA}}[-\log p_{\theta}^{\text{sparse}}(t)]$ and $\mathbb{E}_{\text{FA}}[-\log p_{\theta}^{\text{full}}(t)]$ are the expected NLL based on full attention trained model but using sparse/full attention in inference stage regarding a specific generation result t , respectively.

Then, the KL divergence of p_{θ}^{full} and $p_{\theta}^{\text{sparse}}$ is defined as:

$$\begin{aligned}D_{\text{KL}}\left(p_{\theta}^{\text{full}}(t) \| p_{\theta}^{\text{sparse}}(t)\right) &= \mathbb{E}_{\text{FA}}\left[\log \frac{p_{\theta}^{\text{full}}(t)}{p_{\theta}^{\text{sparse}}(t)}\right] \\ &= \mathbb{E}_{\text{FA}}[-\log p_{\theta}^{\text{sparse}}(t)] - \mathbb{E}_{\text{FA}}[-\log p_{\theta}^{\text{full}}(t)] \\ &= \mathcal{L}_{\text{FA}}^{\text{sparse}}(t) - \mathcal{L}_{\text{FA}}^{\text{full}}(t).\end{aligned}$$

Rearranging terms yields:

$$\mathcal{L}_{\text{FA}}^{\text{sparse}}(t) = \mathcal{L}_{\text{FA}}^{\text{full}}(t) + D_{\text{KL}}\left(p_{\theta}^{\text{full}}(t) \| p_{\theta}^{\text{sparse}}(t)\right).$$

□

B Proof of Theorem 1

Proof. We decompose the full attention output into contributions from selected tokens $\mathcal{S}(t)$ and dropped tokens $\mathcal{S}^c(t)$:

$$h^{\text{full}}(t) = \sum_{j \in \mathcal{S}(t)} a^{\text{full}}(t, j)v(j) + \sum_{j \in \mathcal{S}^c(t)} a^{\text{full}}(t, j)v(j). \quad (10)$$

For any token $j \in \mathcal{S}(t)$, the full and sparse attention weights are related by:

$$a^{\text{full}}(t, j) = \frac{\exp(s(t, j))}{\sum_{k < t} \exp(s(t, k))}, \quad a^{\text{sparse}}(t, j) = \frac{\exp(s(t, j))}{\sum_{k \in \mathcal{S}(t)} \exp(s(t, k))},$$

where $s(t, j)$ denotes the unnormalized attention score from query position t to key position j . Their ratio yields:

$$\frac{a^{\text{full}}(t, j)}{a^{\text{sparse}}(t, j)} = \frac{\sum_{k \in \mathcal{S}(t)} \exp(s(t, k))}{\sum_{k < t} \exp(s(t, k))} = 1 - \delta(t),$$

where $\delta(t) = \sum_{j \in \mathcal{S}^c(t)} a^{\text{full}}(t, j)$ is the dropped attention mass. Thus, for any $j \in \mathcal{S}(t)$:

$$a^{\text{full}}(t, j) = (1 - \delta(t)) a^{\text{sparse}}(t, j). \quad (11)$$

Substituting Eq. (11) into the first term of Eq. (10):

$$\sum_{j \in \mathcal{S}(t)} a^{\text{full}}(t, j)v(j) = (1 - \delta(t)) \sum_{j \in \mathcal{S}(t)} a^{\text{sparse}}(t, j)v(j) = (1 - \delta(t)) h^{\text{sparse}}(t).$$

Substituting back into Eq. (10) and rearranging:

$$h^{\text{full}}(t) - h^{\text{sparse}}(t) = \sum_{j \in \mathcal{S}^c(t)} a^{\text{full}}(t, j)v(j) - \delta(t)h^{\text{sparse}}(t).$$

Taking norms and applying the triangle inequality:

$$\|h^{\text{full}}(t) - h^{\text{sparse}}(t)\| \leq \left\| \sum_{j \in \mathcal{S}^c(t)} a^{\text{full}}(t, j)v(j) \right\| + \delta(t)\|h^{\text{sparse}}(t)\|. \quad (12)$$

For the first term, applying the triangle inequality and using the non-negativity of attention weights:

$$\left\| \sum_{j \in \mathcal{S}^c(t)} a^{\text{full}}(t, j)v(j) \right\| \leq \sum_{j \in \mathcal{S}^c(t)} a^{\text{full}}(t, j)\|v(j)\| \leq \delta(t) \max_{j \in \mathcal{S}^c(t)} \|v(j)\|.$$

Substituting into Eq. (12) and factoring out $\delta(t)$ yields the result:

$$\|h^{\text{full}}(t) - h^{\text{sparse}}(t)\| \leq \delta(t) \left(\max_{j \in \mathcal{S}^c(t)} \|v(j)\| + \|h^{\text{sparse}}(t)\| \right).$$

□

Algorithm 1 SSA Dual-Stream Training with A Bi-directional Alignment

```

Input: embeddings  $x_0$ , targets  $y$ , number of layers  $L$ , alignment weight  $\alpha$ , routing prob.  $p_{\text{FA}}$ 
if training then
    goFA  $\leftarrow$  Bernoulli( $p_{\text{FA}}$ )
else
    goFA  $\leftarrow$  False
end if
MainAttn  $\leftarrow$  FullAttn if goFA else SparseAttn
AuxAttn  $\leftarrow$  SparseAttn if goFA else FullAttn
 $x \leftarrow x_0$ ;  $\mathcal{L}_{\text{align}} \leftarrow 0$ 
for  $l = 1$  to  $L$  do
     $h \leftarrow \text{Norm1}_l(x)$ 
     $q \leftarrow Q_l(h)$ ;  $k \leftarrow K_l(h)$ ;  $v \leftarrow V_l(h)$ 
     $h_{\text{main}} \leftarrow \text{MainAttn}(q, k, v)$ 
     $h_{\text{aux}} \leftarrow \text{AuxAttn}(q, k, v)$ 
     $\mathcal{L}_{\text{sparse}} \leftarrow \|h_{\text{main}} - \text{sg}(h_{\text{aux}})\|$ 
     $\mathcal{L}_{\text{commit}} \leftarrow \|h_{\text{aux}} - \text{sg}(h_{\text{main}})\|$ 
     $\mathcal{L}_{\text{align}} \leftarrow \mathcal{L}_{\text{align}} + \mathcal{L}_{\text{sparse}} + \mathcal{L}_{\text{commit}}$ 
     $x \leftarrow x + O_l(\text{Gate}_l(h) \odot h_{\text{main}})$ 
     $h \leftarrow \text{Norm2}_l(x)$ 
     $x \leftarrow x + \text{FFN}_l(h)$ 
end for
 $\mathcal{L}_{\text{align}} \leftarrow \mathcal{L}_{\text{align}}/L$ ;  $x \leftarrow \text{LayerNorm}(x)$ 
logits  $\leftarrow \text{LMHead}(x)$ 
if training then
     $\mathcal{L}_{\text{ce}} \leftarrow \text{CrossEntropy}(\text{logits}, y)$ 
    return logits,  $\mathcal{L}_{\text{ce}} + \alpha \cdot \mathcal{L}_{\text{align}}$ 
else
    return logits
end if

```

C Implementation Details

The model configurations are summarized in Table A1. We adopt the open-source NSA implementation³ and use the Liger Kernel [39] for acceleration.

We annotate the two minor modifications: (1) We reduce the number of key-value heads to 2 to adapt block-sparse attention implementation and accelerate training; (2) We adopt Gated Attention [19] to mitigate the attention sink-this mechanism is also implicitly employed in NSA [11]-so we apply this gating mechanism to all methods for fair comparison.

Table A1. Model configurations for the 1B and 300M parameter models.

Config Field	1B Model	300M Model
Block Size	16	16
Block Counts	16	16
Hidden Size	2048	1024
Intermediate Size	8192	4096
Num Hidden Layers	16	16
Num Attention Heads	32	16
Num KV Heads	2	1
Head Dim	64	64
Max Position Embeddings	131072	131072
Vocabulary Size	128256	128256
BOS Token	128000	128000
EOS Token	128001	128001
RMSNorm Eps	1e-5	1e-5
Hidden Activation	SiLU	SiLU
Attention Bias	false	false
MLP Bias	false	false
Attention Dropout	0.0	0.0
Initializer Range	0.02	0.02
Pretraining TP	1	1
Tie Word Embeddings	true	true
Torch Dtype	bfloat16	bfloat16
RoPE Base θ	500,000	500,000
<i>RoPE Scaling (Long Context Evaluation Only)</i>		
Scaling Factor	4.0	4.0
Low / High Freq Factor	1.0 / 4.0	1.0 / 4.0
Scaling Type	llama3	llama3
Original Max Position	8192	8192

³<https://github.com/fla-org/native-sparse-attention>

D Efficiency Analysis

We report training and inference time statistics in Table A2 and Table A3, respectively.

For training, FullAttn achieves the shortest time due to its highly optimized implementation. SSA incurs only 17% more time than MoBA, indicating that the dynamic attention computation in each layer introduces minimal overhead. Interestingly, the pre-training time for RF=256 is shorter than that for RF=1024, but this trend reverses during continual training. This can be explained by the two-stage computation in sparse attention: the first stage computes block-level attention scores without softmax, and the second stage computes attention over the selected tokens. Denoting the number of tokens involved in each stage as N and M , we can approximate the computational complexity as $N^2 + M^2$. As shown in Table A4, this analysis explains the observed efficiency patterns.

At inference, SSA matches MoBA’s speed under sparse mode and equals FullAttn when full attention is triggered. While the sparse mode offers a modest gain at 8k, the advantage widens as context grows—delivering 2x speed-up at 128k length.

Table A2. Wall clock time (GPU-Hours) comparison for training different attention mechanisms. SSA incurs only slightly higher training time (< 18%) than MoBA.

Method	Receptive Field	Pre-training (8k)	Continual (32k)
FullAttn	-	792	112
MoBA	256	856	136
	1024	928	128
NSA	256	976	160
	1024	1040	144
SSA	256	1008	176
	1024	1088	168

Table A3. Wall clock time (ms) comparison for different attention mechanisms during inference. Sparse attention achieves noticeable speedup at longer context lengths, despite less optimized implementations. Measured for batch size of 1 averaged over 30 runs.

Method	RF Config	8k	16k	32k	64k	128k
FullAttn	—	204.9	356.3	798.3	2178.7	7029.2
Sparse Attention	RF=256	198.1	327.2	674.9	1723.9	5138.0
	RF=1024	199.5	317.0	595.2	1321.8	3411.9
NSA	RF=256	202.6	336.8	695.3	1771.4	5204.1
	RF=1024	204.8	326.7	621.0	1365.4	3495.9

Table A4. Computational complexity of different sparse attention configurations under varying context lengths.

Context Length	Receptive Field	#Block-level Tokens	#Selected Tokens	Approx. Complexity
8192	256	512	256	327k
8192	1024	256	1024	1.11M
32768	256	2048	256	4.26M
32768	1024	1024	1024	2.1M

E Evaluation and Datasets

The statistics and n-shot samples used is shown in Table A5. The dataset statistics and few-shot configurations are summarized in Table A5. For reproducibility, we use fixed random seeds (1, 12, 123, 1234, and 12345) across the five runs on commonsense reasoning benchmarks. For LongBench and NIAH, we use greedy decoding and report results from a single run due to computational constraints—our sparse attention kernel does not currently support KV caching, resulting in slow decoding. Note that NIAH results may vary slightly across runs as the evaluation data is synthesized dynamically.

For perplexity evaluation, we use 1m-evaluation-harness for Wikitext, reporting word-level perplexity as implemented by the framework. For PG-19 long-context perplexity, we implement sliding-window evaluation with a stride of 256 [36, 37]. Due to the large number of samples, we evaluate on 1000 randomly selected samples using seed 42 and convert the loss to perplexity directly via the exponential relation.

Table A5. Evaluation Benchmark Statistics

Evaluation Benchmark	N-Shot	Data Size
PIQA	3	1,838
Hellaswag	10	10,042
ARC-Easy	25	2,376
ARC-Challenge	5	1,172
LongBench	-	4,750
Needle-in-A-Haystack	-	500 cases per test

Table A6. NSA extrapolated to full attention results. `cmp`, `fa`, and `swa` denote compression, full attention, and sliding window, respectively. We do not evaluate the commonsense reasoning for those methods exploding the perplexity.

Configuration	PIQA	HellaSwag	ARC-E	ARC-C	AVG	Wiki8K
<code>cmp+fa+swa</code>	73.24	58.13	70.13	37.06	59.64	15.86
<code>cmp+fa+fa</code>	—	—	—	—	—	60.88
<code>fa+fa+swa</code>	—	—	—	—	—	72.05
<code>fa+fa+fa</code>	—	—	—	—	—	191.3

F NSA Is Not Suitable for Full Attention Evaluation

NSA aggregates outputs from three independent sparse attention modules, each capturing information at different levels: (1) **Compression**: maintains a compressed representation with a full view of all preceding tokens; (2) **Selection**: a top- k block selection module that operates identically to MoBA; and (3) **Sliding Window**: a local attention module that attends to the most recent tokens. Excluding any module would impair performance due to distribution mismatch.

In principle, all three modules can be extrapolated to full attention. However, as shown in Table A6, replacing all three with full attention (`fa+fa+fa`) yields extremely high perplexity (191.3). To identify which modules fail to extrapolate, we test three additional configurations: `cmp+fa+swa`, `cmp+fa+fa`, and `fa+fa+swa` as we already know the selection module can be extrapolated to full attention well. The results show that only the selection module extrapolates well to full attention, and the compression and sliding window modules both fail. Considering that two out of three modules cannot extrapolate reliably, we exclude NSA from full attention inference evaluation.

G NSA with and without Sliding Window

We investigate whether NSA’s strong perplexity performance stems from its sparse attention mechanism or its sliding window component, which is not used in other sparse attention methods. In our experiments, NSA is trained with a receptive field of 256 tokens, while the sliding window size is 128 tokens. As shown in Table A7, removing the sliding window leads to degradation across most downstream tasks, with notable drops in Hellaswag (-1.18) and ARC-E (-1.1). More critically, Table A8 reveals that without a sliding window, NSA suffers severe perplexity degradation at longer context lengths with RoPE scaling and continual-training, and SSA can consistently outperform NSA without the sliding window. **These results suggest that NSA’s reported perplexity advantages largely depend on the sliding window module, which contributes additional local tokens, rather than its sparse attention design, making direct comparisons with other sparse attention methods that lack this component potentially misleading.**

Table A7. Comparison of NSA with and without the sliding window module on commonsense reasoning and perplexity.

Method	PIQA	Hellaswag	ARC-E	ARC-C	Average	PPL \downarrow
NSA-window	73.23 ± 0.3	58.15 ± 0.32	69.8 ± 0.34	36.71 ± 0.58	59.47 ± 0.2	16.02
NSA-nowindow	73.44 ± 0.43	56.97 ± 0.24	68.7 ± 0.45	36.48 ± 0.53	58.9 ± 0.21	16.3

Table A8. Long-context perplexity after RoPE scaling on PG-19. The best perplexities are **bolded**, and the second best perplexities are underlined. SSA consistently outperforms NSA-nowindow on long-context perplexity evaluation.

Method	4K	8K	16K	32K
NSA-window	15.66	15.33	15.20	15.00
NSA-nowindow	16.29	16.01	15.99	18.16
SSA	<u>16.07</u>	<u>15.78</u>	<u>15.67</u>	<u>15.53</u>
NSA-window-32k-trained	15.93	15.6	15.46	15.21
NSA-nowindow-32k-trained	16.18	15.87	15.73	15.51
SSA-32k-trained	<u>16.01</u>	<u>15.7</u>	<u>15.56</u>	<u>15.32</u>

H KL Divergence

We analyze the relationship between attention approximation quality and downstream performance by measuring two metrics: (1) KL divergence between sparse and full attention at the final layer, and (2) attention sparsity. Table A9 reports these metrics alongside perplexity and average commonsense reasoning scores for SSA, MoBA, and FullAttn. The results show that SSA achieves the smallest KL divergence, which we attribute to the alignment loss.

Table A9. Comparison of KL divergence, attention sparsity, perplexity, and benchmark accuracy for SSA, MoBA, and FullAttn under 1B-parameter settings.

Method	KL Divergence	AttnSparsity		PPL		Commonsense Avg. / %	
		Sparse	Full	Sparse	Full	Sparse	Full
SSA	0.0661	0.677	0.705	15.97	15.28	60.27	60.39
MoBA	0.1024	0.546	0.527	16.54	16.68	58.73	58.86
FullAttn	0.1486	0.610	0.641	17.05	15.13	59.62	60.01

I Sparsity Extrapolation Results

The detailed scores for commonsense reasoning and Longbench are in Table A10 and Table A11 respectively.

Table A10. Commonsense reasoning and perplexity under sparse inference across varying receptive fields. Both MoBA and SSA are trained with RF=256 but extrapolate to larger RFs. Results are averaged over 5 runs with different seeds.

Method	PIQA/%	HellaSwag/%	ARC-Easy/%	ARC-Challenge/%	Average/% \uparrow	Wikitext PPL \downarrow
Sparse Attention Inference (Receptive Field = 512)						
FullAttn	74.30 ± 0.40	58.12 ± 0.16	68.96 ± 0.53	38.34 ± 0.48	59.93	16.09
MoBA	72.79 ± 0.17	56.24 ± 0.19	69.23 ± 0.29	37.20 ± 0.46	58.87	16.36
SSA	74.49 ± 0.40	58.48 ± 0.14	70.08 ± 0.20	38.77 ± 0.66	60.46	15.62
Sparse Attention Inference (Receptive Field = 1024)						
FullAttn	74.30 ± 0.40	58.12 ± 0.15	69.39 ± 0.54	38.34 ± 0.37	60.04	15.53
MoBA	72.79 ± 0.17	56.20 ± 0.18	69.39 ± 0.26	37.44 ± 0.79	58.96	16.41
SSA	74.49 ± 0.40	58.44 ± 0.09	70.08 ± 0.33	38.57 ± 0.66	60.40	15.44
Sparse Attention Inference (Receptive Field = 2048)						
FullAttn	74.30 ± 0.40	58.12 ± 0.16	69.39 ± 0.54	38.28 ± 0.34	60.02	15.23
MoBA	72.79 ± 0.16	56.19 ± 0.17	69.40 ± 0.24	37.46 ± 0.70	58.96	16.55
SSA	74.49 ± 0.40	58.45 ± 0.10	70.08 ± 0.33	38.43 ± 0.51	60.36	15.39
Sparse Attention Inference (Receptive Field = 4096)						
FullAttn	74.30 ± 0.40	58.12 ± 0.16	69.39 ± 0.54	38.28 ± 0.34	60.02	15.15
MoBA	72.63 ± 0.36	56.15 ± 0.19	69.22 ± 0.23	37.25 ± 0.68	58.81	16.59
SSA	74.58 ± 0.47	58.57 ± 0.11	69.99 ± 0.18	38.79 ± 0.51	60.48	15.26

J Full Longbench Results

Only the average scores are reported in Table 3. The full results evaluated in Longbench is in Table A12 and Table A13, respectively.

Table A11. LongBench Evaluation under sparse inference across varying receptive fields. Both MoBA and SSA are trained with RF=256 but extrapolate to larger RFs.

Category	Dataset	Receptive Field = 512			Receptive Field = 1024		
		FullAttn	MoBA	SSA	FullAttn	MoBA	SSA
Single Doc	NarQA	2.09	2.76	3.91	1.96	2.85	2.92
	Qasper	6.76	7.74	7.12	6.85	8.07	7.27
	MFQA	14.97	13.12	15.28	16.72	12.51	16.64
Multi Doc	HotpotQA	5.50	7.06	6.94	5.80	6.93	7.10
	2WikiQA	8.77	9.71	9.79	8.87	9.70	10.18
	MuSiQue	3.58	3.86	4.06	3.85	3.82	3.68
Summary	GovReport	8.17	11.55	9.48	10.15	12.23	9.52
	QMSum	18.28	16.83	17.38	18.60	15.58	17.38
	MultiNews	14.81	12.78	17.06	15.42	14.08	16.49
Few-shot	TREC	28.5	45.5	51.5	32	48	56.5
	TriviaQA	40.88	37.62	48.80	45.77	38.62	50.22
	SAMSum	33.39	23.62	33.78	34.82	19.34	34.28
Synthetic	PsgCount	3.09	3.25	1.29	3.11	3.09	1.03
	PsgRe-en	3.91	3.89	4.22	3.76	4.29	3.94
Code	LCC	30.44	38.97	29.70	32.14	37.23	29.41
	RepoBen	38.58	40.62	39.36	40.39	39.28	39.46
Average \uparrow		16.36	17.33	18.73	17.51	17.23	19.13
Category	Dataset	Receptive Field = 2048			Receptive Field = 4096		
		FullAttn	MoBA	SSA	FullAttn	MoBA	SSA
Single Doc	NarQA	1.96	2.50	4.60	2.77	1.30	5.06
	Qasper	7.13	7.05	7.59	7.24	5.88	6.72
	MFQA	16.77	12.86	15.45	16.69	12.04	16.41
Multi Doc	HotpotQA	6.05	7.01	7.13	6.89	6.56	7.54
	2WikiQA	8.52	8.83	10.26	10.35	8.10	9.58
	MuSiQue	3.94	4.25	3.76	3.81	3.49	3.98
Summary	GovReport	10.77	12.29	10.09	11.81	11.93	9.35
	QMSum	17.85	14.12	17.76	16.99	9.73	18.11
	MultiNews	14.81	13.83	16.03	14.73	13.80	15.06
Few-shot	TREC	37.5	44.5	54	41	39	55.5
	TriviaQA	46.29	38.66	51.00	46.17	35.47	48.62
	SAMSum	33.45	13.50	34.47	34.14	9.86	33.76
Synthetic	PsgCount	3.09	2.84	1.19	3.28	2.41	1.30
	PsgRe-en	3.56	3.75	4.34	3.68	4.21	3.89
Code	LCC	31.98	37.51	29.29	32.03	37.10	29.05
	RepoBen	39.74	38.33	39.24	38.57	37.07	39.54
Average \uparrow		17.78	16.38	19.14	18.13	14.87	18.97

Table A12. LongBench evaluation with per-dataset scores for length extrapolated models with RoPE scaling.

Category	Dataset	Full			Receptive Field = 256				Receptive Field = 1024			
		FA	MoBA	SSA	FA	MoBA	NSA	SSA	FA	MoBA	NSA	SSA
Single Doc	NarQA	2.02	1.33	3.41	1.89	4.12	2.31	2.45	2.01	3.24	3.2	3.23
	Qasper	7.46	5.82	7.19	5.84	7.52	7.06	6.12	6.9	6.52	6.58	6.69
	MFQA	16.77	11.26	16.33	14.24	13.75	13.62	16.66	15.91	15.14	16.99	15.6
Multi Doc	HotpotQA	7.37	6.02	6.88	5.29	6.42	7.03	6.42	5.23	6.04	6.35	6.43
	2WikiQA	10.18	7.36	10.24	8.99	9.64	9.5	10.03	8.78	8.74	8.9	10.71
	MuSiQue	3.97	3.62	3.69	3.46	3.49	4.86	3.57	2.98	3.43	4.11	3.34
Summary	GovReport	11.48	12.18	8.76	6.69	10.24	10.57	9.1	8.82	6.33	9.76	8.6
	QMSum	15.36	5.55	17.12	17.85	17.7	18.83	17.06	18.24	17.67	18.13	17.81
	MultiNews	14.66	14.04	15.13	12.84	13.05	12.39	15.26	15.13	11.01	8.58	16.41
Few-shot	TREC	41	34	49.5	19	40	39.5	48.5	28.5	47.5	34.5	52
	TriviaQA	44.18	29.39	48.85	35.88	37.55	37.54	44.72	41.83	46.64	46.88	48.75
	SAMSum	31.56	9.01	33.39	30.51	23.74	30.51	32.57	33.93	35.07	31	33.27
Synthetic	PsgCount	3.17	1.99	1.07	3.18	3.32	3.3	0.97	3.14	1.02	3.18	1.27
	PsgRe-en	3.53	3.11	4.03	3.74	2.75	3.4	3.42	4.07	4.58	3.38	4.01
Code	LCC	32.75	37.16	29.05	29.97	38.19	36.56	29.5	31.97	37.21	35.82	29.35
	RepoBen	37.93	36.1	38.52	36.67	38.52	38.98	39.83	40.11	41.51	40.45	39.75
Average ↑		17.71	13.62	18.32	14.75	16.88	17.25	17.89	16.72	18.23	17.36	18.58

Table A13. LongBench evaluation with per-dataset scores for continual-trained models.

Category	Dataset	Full			Receptive Field = 256				Receptive Field = 1024			
		FA	MoBA	SSA	FA	MoBA	NSA	SSA	FA	MoBA	NSA	SSA
Single Doc	NarQA	2.35	2.24	4.87	1.92	3.66	2.32	4.61	1.88	4.5	2.41	3.71
	Qasper	8.31	6.64	7.77	5.12	6.95	7.23	6.54	7.54	7.59	7.21	7.42
	MFQA	19.15	11.3	15.95	13.78	13.54	14.04	15.45	14.87	15.93	16.73	15.8
Multi Doc	HotpotQA	7	6.22	7.56	5.14	6.2	6.47	6.25	5.24	6.76	6.74	6.69
	2WikiQA	8.14	7.71	11	9.18	9.65	8.5	9.83	9.39	9.23	9.17	10.03
	MuSiQue	3.63	3.44	3.77	3.22	3.8	4.04	3.82	3.46	3.64	3.89	3.38
Summary	GovReport	12.3	12.09	12.41	7	10.48	12.25	9.94	8.52	9.32	12.53	10.61
	QMSum	18.78	4.96	18.17	18.72	19.15	19.7	17.87	18.73	17.73	17.65	18.42
	MultiNews	15.72	14.03	20.43	12.95	12.8	13.59	16.87	16.51	12	12.3	19.95
Few-shot	TREC	49.5	40	52	25.5	42	41.5	48.5	31.5	48	38.5	50.5
	TriviaQA	46.98	32.96	50.45	35.08	37.23	38.67	46.24	40.63	45.65	50.01	49.67
	SAMSum	35.27	11.39	34.89	30.21	24.56	32.2	33.23	34.25	35.56	32.54	34.34
Synthetic	PsgCount	3.02	1.74	0.85	3.18	3.52	3.2	0.69	3.21	0.71	3.18	0.87
	PsgRe-en	3.96	3.08	3.8	3.16	4.1	3.48	3.95	5.06	5	3.92	3.4
Code	LCC	30.31	35.97	28.67	27.84	37.65	33.96	29.13	29.98	36.12	32.63	29.13
	RepoBen	39.14	37.68	40.21	37.43	39.43	38.12	39.12	38.65	41.14	39.84	40.9
Average ↑		18.97	14.47	19.55	14.96	17.17	17.45	18.25	16.84	18.68	18.08	19.05

K Further Ablations

Alpha. We observe that different weightings α (the coefficient of the alignment loss) affect performance, as they control the relative strength of the two loss terms (Table A14). It is necessary to balance the objectives.

Alignment Loss Type. We also experimented with L2 loss in addition to SmoothL1 loss. Rather than tuning α , we simply downscaled it from 10 to 5 based on the initial scale of the alignment loss relative to the cross-entropy loss. With this minimal adjustment, L2 performs slightly below our default SSA configuration. However, even this variant outperforms MoBA, suggesting that the choice of distance metric is flexible and any reasonable alignment loss should work for SSA.

Table A14. Additional ablation studies.

Method	PPL \downarrow	Comm. Avg. \uparrow
Baseline (SSA)	24.20	49.69
MoBA	24.51	48.81
Alpha		
$\alpha = 5$	24.16	48.71
$\alpha = 10$ (Baseline)	24.20	49.69
$\alpha = 20$	24.31	49.45
Alignment Loss Type		
L2 Loss	24.31	49.27

L Sparse Attention is Robust to RoPE Scaling

RoPE scaling prevents perplexity explosion beyond the pre-trained context window (Figure 4a) by extending the periods of low-frequency bands, thereby eliminating aliasing (see Appendix L.1 for details). However, this scaling impairs overall perplexity by distorting the learned frequency representations. Interestingly, sparse attention is more robust to this degradation. Figure 4 shows that perplexity degradation follows: sparse 256 tokens $<$ sparse 1024 tokens $<$ full attention. We attribute this to two factors. First, sparse attention attends to fewer tokens overall, limiting cumulative exposure to distorted positional encodings. Second, the selected tokens are skewed toward local context (<8k positions) (Appendix L.2 and Figure A4), where RoPE scaling induces less distortion.

L.1 Aliased Frequency Bands in Length Extrapolation

When a pre-trained model is directly applied to a 32k context length without adaptation, its attention distribution exhibits anomalous patterns—sometimes manifesting as dual peaks in the middle of the context, as shown in Figure A1. This phenomenon is distinct from the well-known attention sink problem. Examining the QK product (i.e., the logits before softmax) in Figure A2 reveals a clear periodic wave pattern, which arises from frequency aliasing in RoPE’s positional encoding. The root cause lies in the model’s limited exposure during training. When trained on 8k contexts, the model never observes how certain frequency bands behave at longer distances. Specifically, frequency bands that appear non-periodic within 8k positions become periodic when extrapolated to 32k, as illustrated in Figure A3. This aliasing causes the model to perceive distant positions as “local,” leading to the perplexity explosion beyond 8k shown in Figure 4. RoPE scaling resolves this issue by stretching the periods of low-frequency bands by a factor of 4 (Table A15). Consequently, frequency bands that were non-periodic within 8k remain non-periodic at 32k, eliminating the aliasing artifacts visible in Figures A1 and A2.

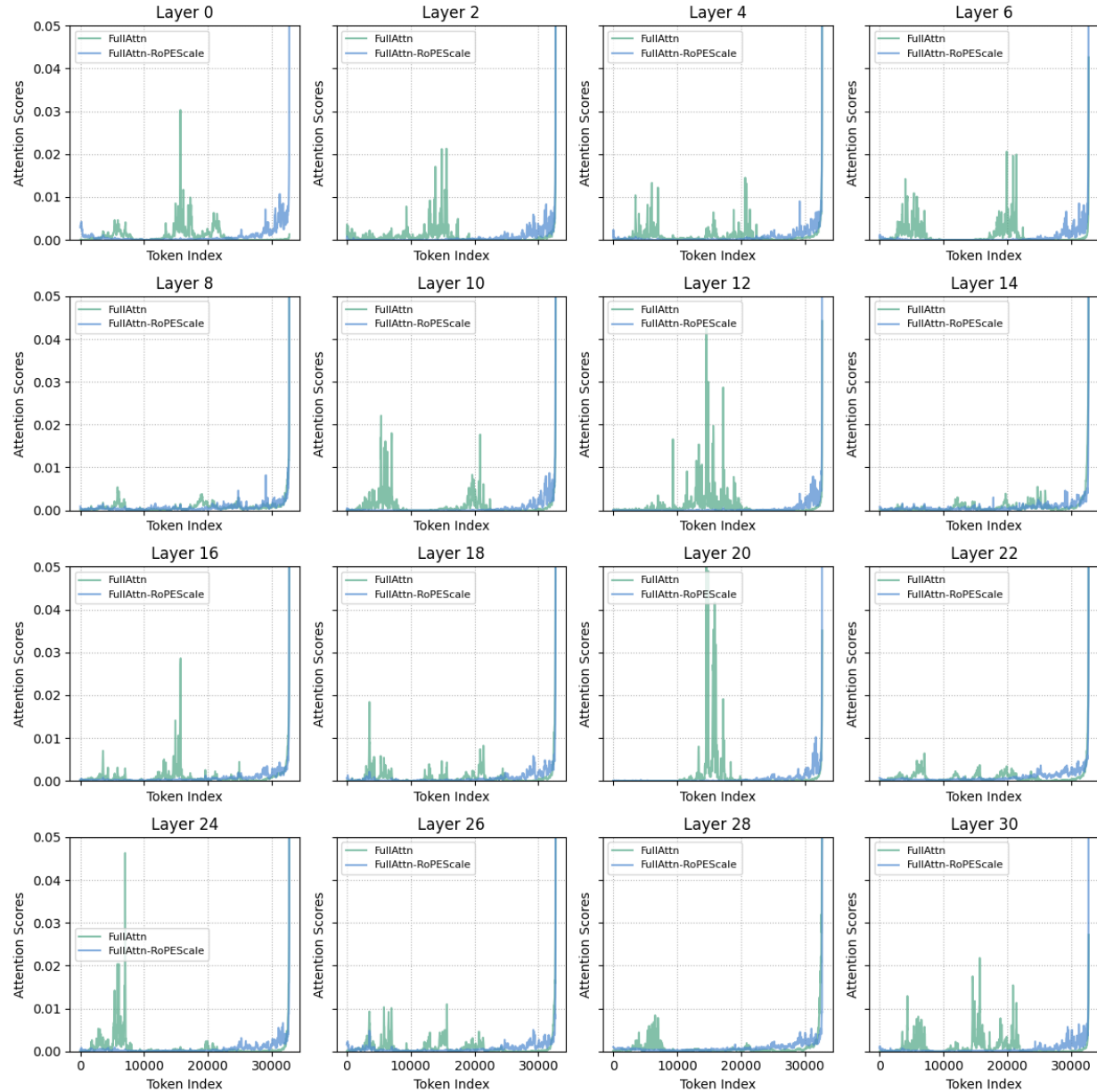


Figure A1. Attention score distributions for FullAttn and FullAttn with RoPE scaling at a context length of 32k.

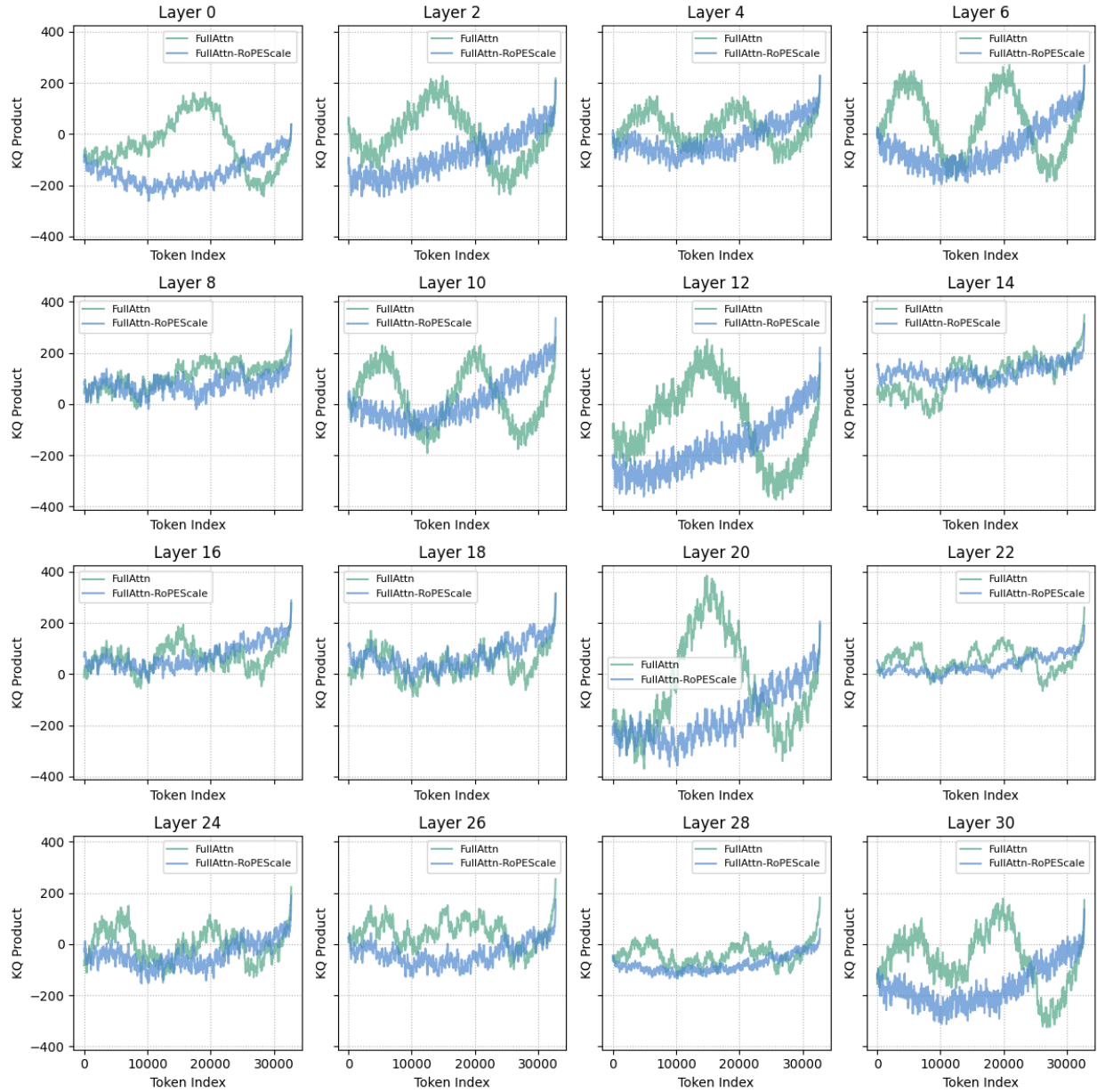


Figure A2. The KQ Product distributions for FullAttn and FullAttn with RoPE scaling at a context length of 32k. The KQ Product is the value before the softmax operation when calculating the attention.

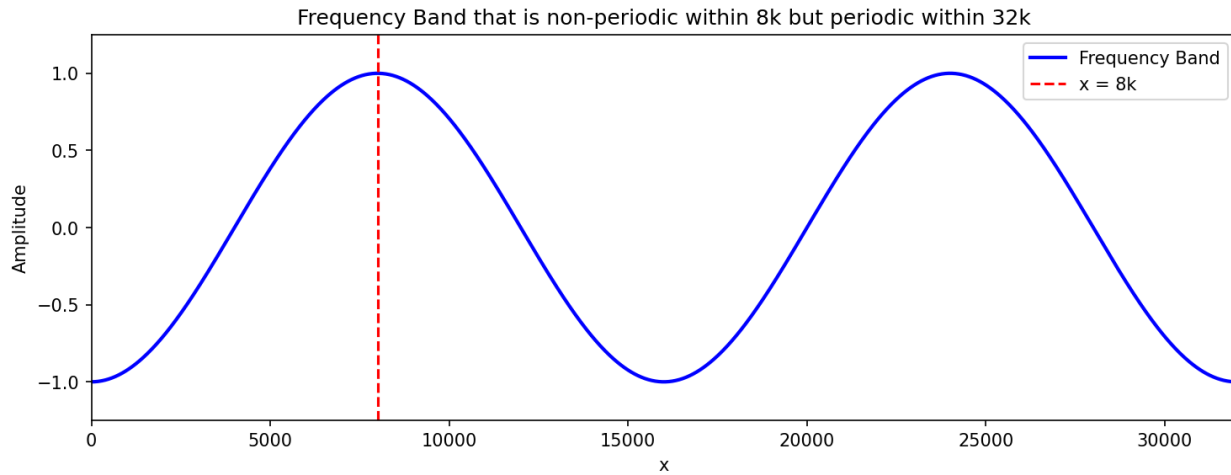


Figure A3. A Frequency Band that is non-periodic within the pre-training length, yet is periodic under a longer length.

Table A15. RoPE frequency periods before and after scaling.

Dimension	Before Scaling	After Scaling
0	6.28×10^0	6.28×10^0
1	9.47×10^0	9.47×10^0
2	1.43×10^1	1.43×10^1
3	2.15×10^1	2.15×10^1
4	3.24×10^1	3.24×10^1
5	4.88×10^1	4.88×10^1
6	7.36×10^1	7.36×10^1
7	1.11×10^2	1.11×10^2
8	1.67×10^2	1.67×10^2
9	2.52×10^2	2.52×10^2
10	3.79×10^2	3.79×10^2
11	5.72×10^2	5.72×10^2
12	8.62×10^2	8.62×10^2
13	1.30×10^3	1.30×10^3
14	1.96×10^3	1.96×10^3
— Period = 2048: Below unscaled, above linearly interpolated —		
15	2.95×10^3	4.24×10^3
16	4.44×10^3	9.64×10^3
17	6.70×10^3	2.19×10^4
— Period = 8192: Above scaled by factor 4× —		
18	1.01×10^4	4.04×10^4
19	1.52×10^4	6.08×10^4
20	2.29×10^4	9.16×10^4
21	3.45×10^4	1.38×10^5
22	5.20×10^4	2.08×10^5
23	7.84×10^4	3.14×10^5
24	1.18×10^5	4.73×10^5
25	1.78×10^5	7.12×10^5
26	2.68×10^5	1.07×10^6
27	4.04×10^5	1.62×10^6
28	6.09×10^5	2.44×10^6
29	9.18×10^5	3.67×10^6
30	1.38×10^6	5.53×10^6
31	2.08×10^6	8.34×10^6

L.2 Local Token Preference for Long Context

We compute the distribution of distances between selected keys and the current query token for FullAttn (Figure A4), MoBA (Figure A5), and SSA (Figure A6). All three methods exhibit a preference for local tokens, which are less affected by RoPE scaling in lower frequency bands. We also compute sparsity and entropy for FullAttn, MoBA, and SSA under four different context lengths with RoPE scaling, as shown in Table A16. SSA consistently achieves higher sparsity and lower entropy.

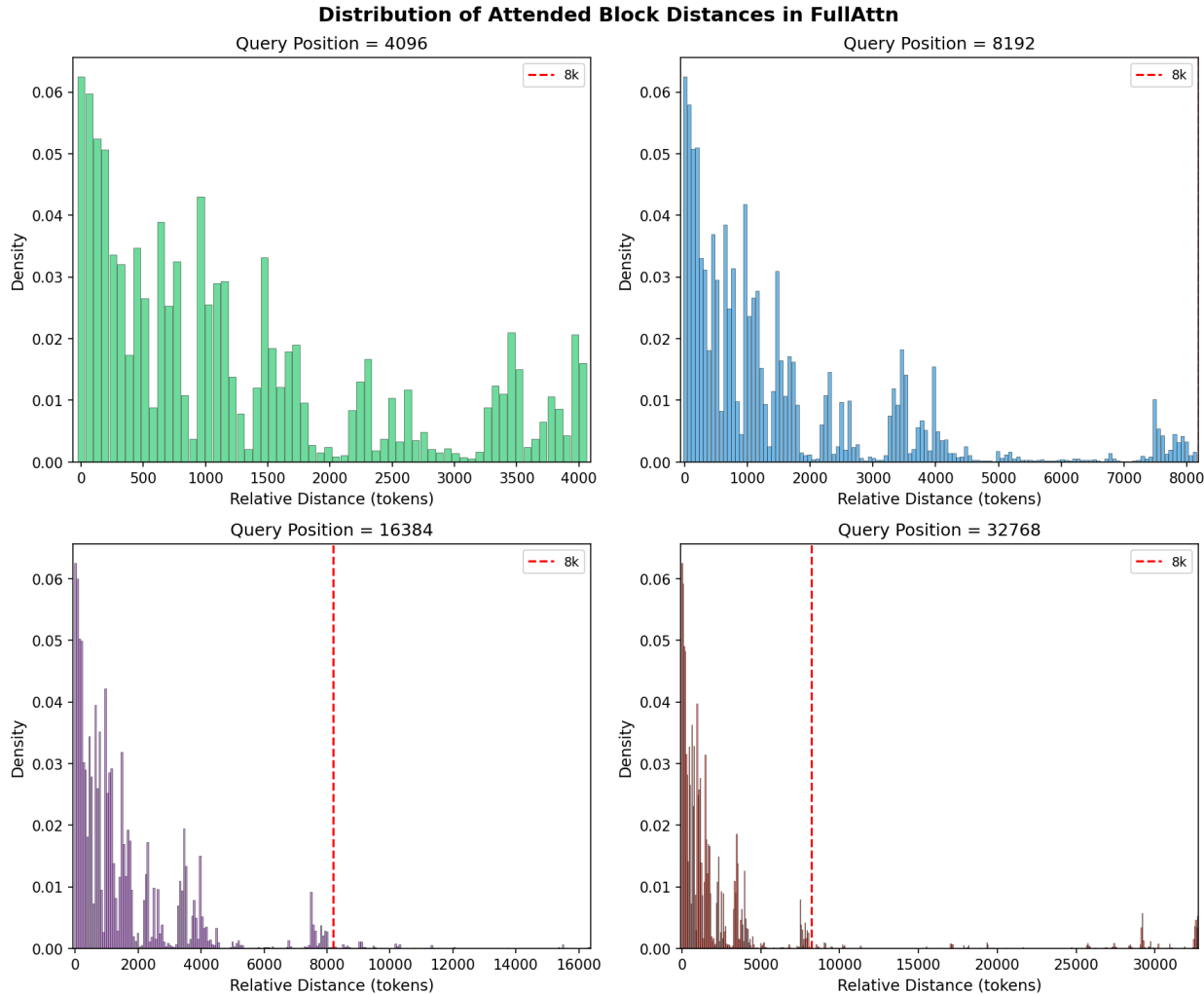


Figure A4. The histogram of the distance from the attended token to the query for FullAttn in sparse inference mode.

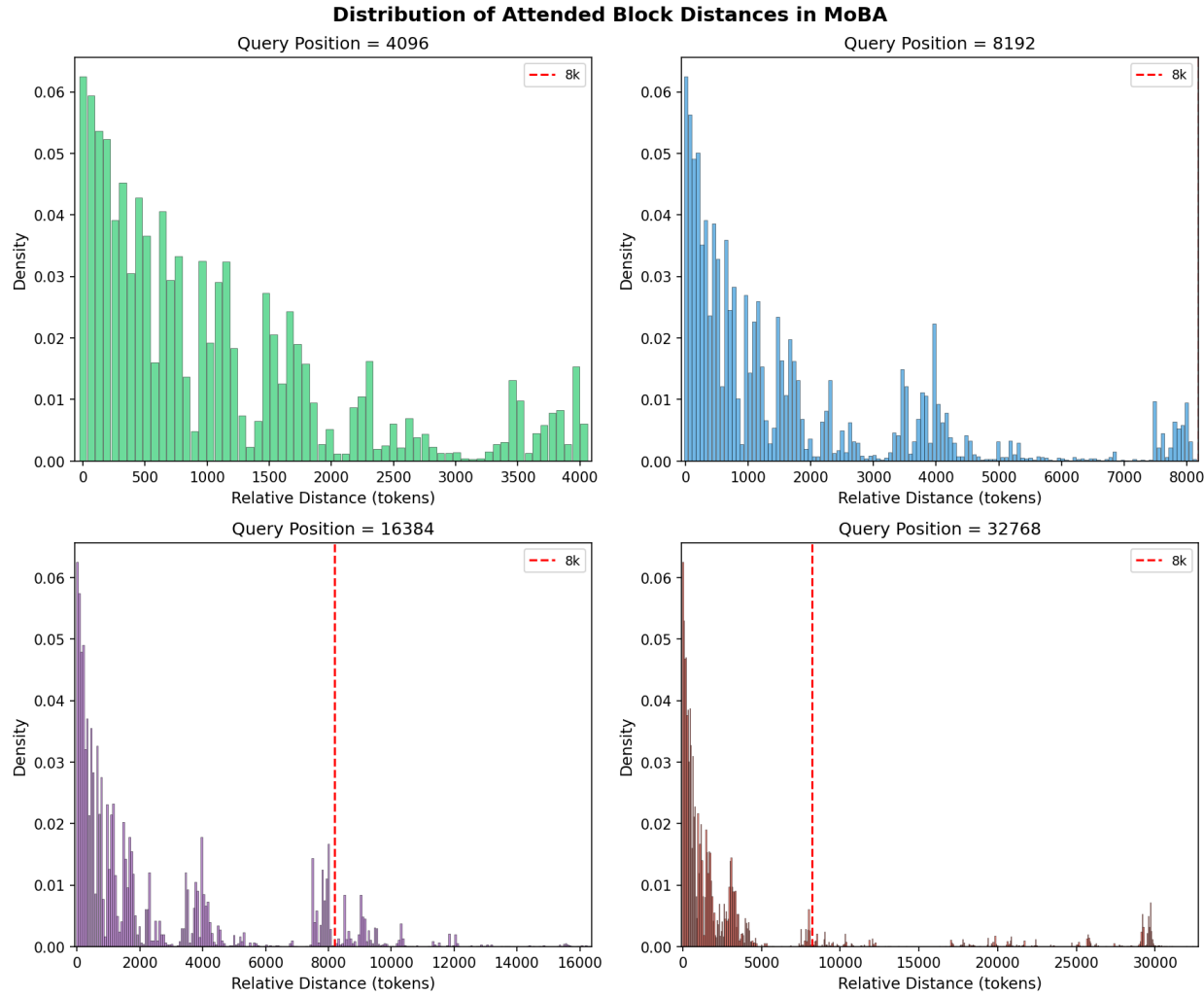


Figure A5. The histogram of the distance from the attended token to the query for MoBA in sparse inference mode.

Table A16. Attention patterns under full attention inference during long-context inference. SSA exhibits consistently sparser attention patterns.

Context	Method	AttnSparsity \uparrow	AttnEntropy \downarrow
4k	FullAttn	0.612	8.89
	MoBA	0.606	9.01
	SSA	0.782	7.63
8k	FullAttn	0.553	9.49
	MoBA	0.541	9.69
	SSA	0.737	8.07
16k	FullAttn	0.543	9.70
	MoBA	0.490	10.28
	SSA	0.714	8.28
32k	FullAttn	0.511	10.21
	MoBA	0.423	11.30
	SSA	0.707	8.51

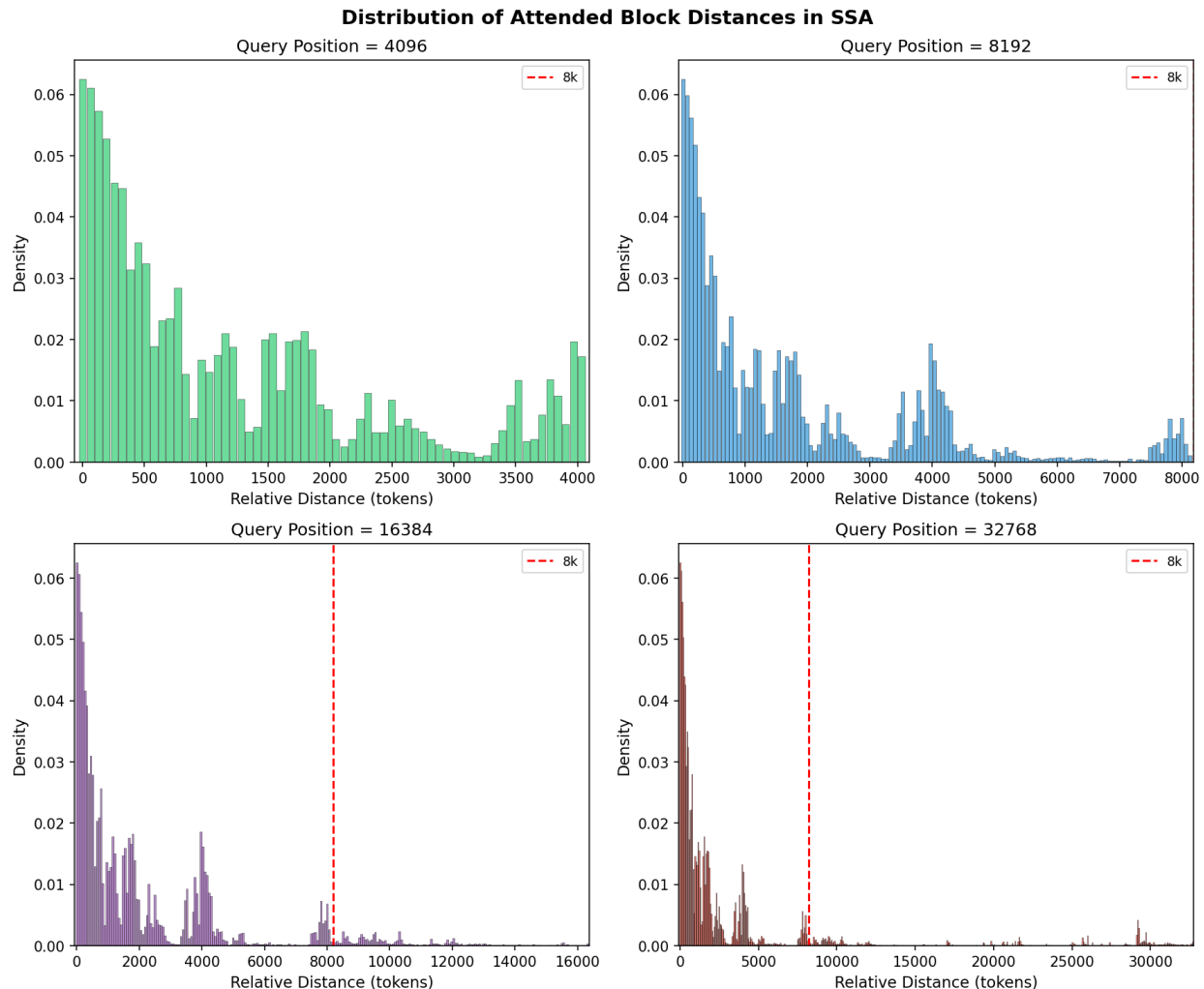


Figure A6. The histogram of the distance from the attended token to the query for SSA in sparse inference mode.